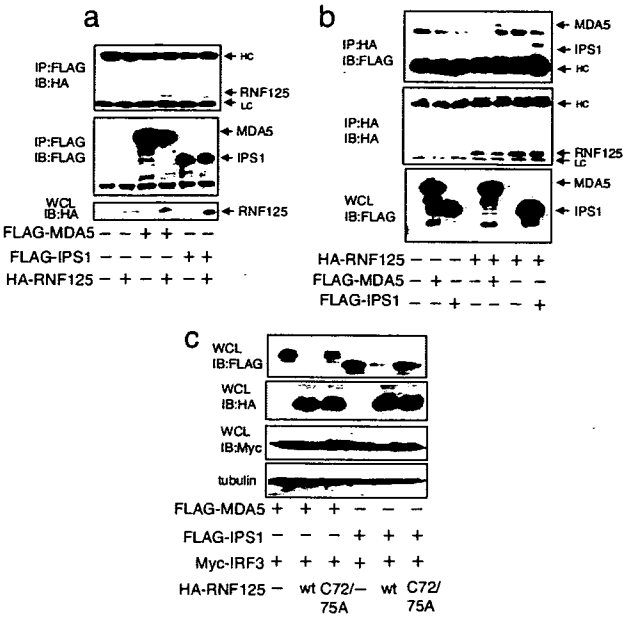

Fig. 5. Association of RNF125 with MDA5 and IPS-1. A plasmid encoding FLAG-MDA5 or FLAG-IPS1 was transfected into 293FT cells in the presence or absence of a plasmid encoding HA-RNF125. (*a* and *b*) Protein–protein interactions were monitored by coimmunoprecipitation using the anti-FLAG antibody, followed by Western blot with the anti-HA antibody (*a*) and coimmunoprecipitation using the anti-HA antibody, followed by Western blot with the anti-FLAG antibody (*b*). All cells were grown in medium containing MG132. (*c*) MDA5 and IPS1 were also degraded by RNF125. A plasmid encoding Myc-IRF3 and FLAG-MDA5 or FLAG-IPS1 were transfected into 293FT cells with or without a plasmid encoding HA-RNF125 or HA-RNF125 C72/75A. Thirty-six hours after transfection, cells were harvested and were analyzed for protein levels by Western blot.

through its CARD domain. These proteins are associated with RNF125 (Fig. 5 *a* and *b*). The concentrations of MDA5 and IPS1 were observed to reduce in cells expressing RNF125 ectopically (Fig. 5*c*). Furthermore, we noticed that these proteins were ubiquitin-conjugated by RNF125, and not by the RNF125 mutant, although the levels of conjugation differed between the substrates (SI Fig. 8 *a* and *b*). Suppression of conjugation of ubiquitin to these proteins was observed by treatment with siRNA specific to RNF125 (SI Fig. 8 *a* and *b Right*). Bringing all these data together, RNF125 serves as a ubiquitin E3-ligase for MDA5 and IPS1 as well as for RIG-I.

Analyzing a candidate E2 enzyme for ubiquitin conjugation to MDA5 and IPS1 by RNF125 in an *in vitro* assay, we observed that UbcH1 and UbcH5a-c were also involved in the process (SI Fig. 8*c*).

Signaling from MDA5 as Well as from IPS1 Was Suppressed by RNF125 Ubiquitin Conjugation-Dependent Manner. Effect of conjugation of ubiquitin to MDA5 and IPS1 by RNF125 on their downstream signaling was analyzed by luciferase assay. Cells were transfected with plasmids expressing IFNβ-luc, MDA5, or IPS1 together with that expressing RNF125 or its mutant. The luciferase activities in cells expressing MDA5 and IPS1 were severely impaired by the expression of RNF125, and not by Δ76 (SI Fig. 9 *a* and *b*). Alternatively, those cells treated with siRNF125–3 showed increased activity of luciferase in the cells bearing both MDA5 and IPS1 (SI Fig. 9 *a* and *b*). Luciferase activity driven by p53-binding promoter was not affected in cells expressing ectopic p53 and RNF125 (SI Fig. 9*c*).

Discussion

We demonstrated that RIG-I is ubiquitinated before its proteasome-dependent degradation. The RNF125 functioned as an E3-ligase for this conjugation process, because ectopic expression of RNF125 enhanced (Fig. 2*a*) and suppression of endogenous RNF125 by siRNA severely impaired the ubiquitin conjugation of RIG-I (Fig. 2*b*). The RNF125, a RING finger-containing protein (25), also known as TRAC-1, exerts a positive regulatory role on T cell activation. Expression of RNF125/TRAC-1 is higher in lymphoid tissues but is also expressed in a variety of other tissues. The role of RNF125 described here appears to be distinct from that previously reported.

It can be observed that the N-terminal region of RIG-I, the region containing the CARD domain, was conjugated to ubiquitin, by minimal incorporation of ubiquitin to the C-terminal half of RIG-I (Fig. 2*c*). Conjugation was enhanced after the deletion of the C-terminal portion of RIG-I, which contained the helicase domain, a result that is consistent with the earlier postulation that the C terminus of RIG-I may mask the function of the N-terminal region (9).

The MDA5, an RIG-I family member, and IPS1, the downstream signaling proteins that interact with RIG-I via the RIG-I CARD, interacted with RNF125 and were also ubiquitin conjugated (Fig. 5 *a* and *b* and SI Fig. 8 *a* and *b*). These results suggest that RNF125 is a ubiquitin E3-ligase with activity against proteins containing CARD domains. These two ubiquitin-conjugated proteins also underwent proteasomal degradation (Fig. 5*c*). We noticed that MDA5 was ubiquitin-conjugated less than RIG-I by RNF125, but the level of this proteins decreased substantially (Fig. 5*c*). We do not know the reason for this, but there may be the possibility that a small amount of ubiquitination to MDA5 may be sufficient to trigger the degradation or that there is a pathway other than ubiquitin-dependent proteasomal degradation for MDA5 degradation. These observations suggest that ubiquitination of RIG-I/MDA5 and IPS1 inhibits RIG-I signaling by shunting these proteins toward proteasomal degradation. Given that the production of cytokines affects a wide variety of responses in innate and acquired immunity, activation of RIG-I signaling by viral pathogens is quite likely to be strictly controlled. Suppression of endogenous RNF125 levels by siRNA enhanced luciferase activity driven by the IFNβ promoter and up-regulated IFNβ expression (Fig. 3*c*), which clearly demonstrates that RNF125 functions as a negative regulator of RIG-I signaling. Importantly, the negative regulatory function of RNF125 is inversely related to IFN signaling in cells, a factor most likely contributing to the down-regulation of IFN levels as the viral infection resolves.

The suppression of IRF3 signaling by RNF125 was not limited to cultured cell lines, but was also seen in primary MEFs (Fig. 3*d*), in which RIG-I is the primary factor activating IRF3 during RNA virus infection (35). These results clearly indicate that RNF125 plays an important role in suppressing RIG-I signaling in physiologically immunocompetent cells.

The IFNα and Poly I:C treatment transiently up-regulated RIG-I levels, which peaked at 12 h after the treatment of HepG2 cells (Fig. 4*a*). Reductions in RIG-I expression correlated with the induction of RNF125 and UbcH5, suggesting that these proteins may enhance the degradation of RIG-I by ubiquitin conjugation. This result is found to be consistent with the *in vitro* experiments (Fig. 2 *a* and *b*).

Materials and Methods

Cell Culture, Transfection, and Luciferase Reporter Assays. For details on cell culture, transfection, and luciferase reporter assays, see *SI Methods*.

Yeast Two-Hybrid Screening. Yeast two-hybrid screening was performed as described in *SI Methods*.

Construction of cDNA Expression Plasmids. Expression constructs for RIG-I, MDA5, and IPS-1 have been described (9). Plasmids expressing WT and mutant ubiquitin were obtained from K. Nakayama (Division of Cell Biology, Medical Institute of Bioregulation, Kyushu University, Fukuoka, Kyushu, Japan). WT RNF125 (amino acid 1–232) and mouse RNF125 were cloned into the pCAG vector. To generate point mutants, alanine was substituted for the targeted residues by PCR. The N- and C-terminal truncation mutants (RNF125 1–76 and RNF125Δ76) were generated by standard PCR. The RNF125 and RIG-I were cloned into the pGEX-6P-1 vector (Amersham, Piscataway, NJ) in-frame with an N-terminal GST.

siRNA and Measurement of mRNA. siRNA duplex sequences (siRNF125–3, 5′-CCGUGUGCCUUGAGGUGUU-3′) were custom synthesized by Proligo (Boulder, CO). A control nucleotide, si-control, was purchased from Dharmacon (Lafayette, CO) (nonspecific control duplex IV). mRNA was measured by RT-PCR.

Western Blotting and Immunoprecipitation. Western blotting and immunoprecipitation were done as reported in *SI Methods*.

ELISA. For details on ELISA, see *SI Methods*.

Antibodies and Reagents. Antibodies to FLAG (anti-Flag; M2), HA (12CA5) and HA (3F10) were purchased from Sigma (St. Louis, MO) and Roche (Indianapolis, IN), respectively. Anti-Myc (9E10), anti-IRF3 (FL425) antibody, and anti-ubiquitin antibodies were obtained from Santa Cruz Biotechnology (Santa Cruz, CA). Anti-UbcH5, which reacts with UbcH5a-c, and anti-α tubulin were acquired from Chemicon (Temecula, CA) and Oncogene Research Products (San Diego, CA), respectively. Anti-GST antibodies were purchased from Amersham. Anti-RNF125 polyclonal antibodies were generated in rabbits by using the RNF125 peptide from 215 to 232 aa. Anti-RIG-I monoclonal antibody was described (9). Anti-RIG-I polyclonal antibodies were generated in rabbits by using the RIG-I recombinant protein from 1 to 238 aa. CHX was purchased from Nacalai Tesque (Kyoto, Japan). Poly (I:C) and MG132 were purchased from Amersham and Peptide Institute (Osaka, Japan), respectively.

The GenBank accession number for mRNF125 is AB259692.

We thank Dr. K. I. Nakayama for providing the plasmids expressing the ubiquitin mutants. This work was supported by grants-in-aid for cancer research and for the second-term comprehensive 10-year strategy for cancer control from the Ministry of Health, Labour and Welfare as well as by Grant-in-Aid for Scientific Research on Priority Areas "Integrative Research Toward the Conquest of Cancer" from the Ministry of Education, Culture, Sports, Science and Technology of Japan.

1. Iwasaki A, Medzhitov R (2004) *Nat Immunol* 5:987–995.
2. Theofilopoulos AN, Baccala R, Beutler B, Kono DH (2005) *Annu Rev Immunol* 23:307–336.
3. Takeda K, Akira S (2005) *Int Immunol* 17:1–14.
4. Medzhitov R, Janeway CA, Jr (1997) *Cell* 91:295–298.
5. Janeway CA, Jr, Medzhitov R (2002) *Annu Rev Immunol* 20:197–216.
6. Akira S, Takeda K, Kaisho T (2001) *Nat Immunol* 2:675–680.
7. Takeda K, Kaisho T, Akira S (2003) *Annu Rev Immunol* 21:335–376.
8. Le Bon A, Tough DF (2002) *Curr Opin Immunol* 14:432–436.
9. Yoneyama M, Kikuchi M, Natsukawa T, Shinobu N, Imaizumi T, Miyagishi M, Taira K, Akira S, Fujita T (2004) *Nat Immunol* 5:730–737.
10. Andrejeva J, Childs KS, Young DF, Carlos TS, Stock N, Goodbourn S, Randall RE (2004) *Proc Natl Acad Sci USA* 101:17264–17269.
11. Kawai T, Takahashi K, Sato S, Coban C, Kumar H, Kato H, Ishii KJ, Takeuchi O, Akira S (2005) *Nat Immunol* 6:981–988.
12. Seth RB, Sun L, Ea CK, Chen ZJ (2005) *Cell* 122:669–682.
13. Meylan E, Curran J, Hofmann K, Moradpour D, Binder M, Bartenschlager R, Tschopp J (2005) *Nature* 437:1167–1172.
14. Malakhov MP, Kim KI, Malakhova OA, Jacobs BS, Borden EC, Zhang DE (2003) *J Biol Chem* 278:16608–16613.
15. Schwartz DC, Hochstrasser M (2003) *Trends Biochem Sci* 28:321–328.
16. Zhao C, Beaudenon SL, Kelley ML, Waddell MB, Yuan W, Schulman BA, Huibregtse JM, Krug RM (2004) *Proc Natl Acad Sci USA* 101:7578–7582.
17. Sumpter R, Jr, Loo YM, Foy E, Li K, Yoneyama M, Fujita T, Lemon SM, Gale M, Jr (2005) *J Virol* 79:2689–2699.
18. Morales FC, Takahashi Y, Kreimann EL, Georgescu MM (2004) *Proc Natl Acad Sci USA* 101:17705–17710.
19. Sweet MJ, Leung BP, Kang D, Sogaard M, Schulz K, Trajkovic V, Campbell CC, Xu D, Liew FY (2001) *J Immunol* 166:6633–6639.
20. Chuang TH, Ulevitch RJ (2004) *Nat Immunol* 5:495–502.
21. Kobayashi K, Hernandez LD, Galan JE, Janeway CA, Jr, Medzhitov R, Flavell RA (2002) *Cell* 110:191–202.
22. Nakagawa R, Naka T, Tsutsui H, Fujimoto M, Kimura A, Abe T, Seki E, Sato S, Takeuchi O, Takeda K, *et al.* (2002) *Immunity* 17:677–687.
23. Wang YY, Li L, Han KJ, Zhai Z, Shu HB (2004) *FEBS Lett* 576:86–90.
24. Lin R, Yang L, Nakhaei P, Sun Q, Sharif-Askari E, Julkunen I, Hiscott J (2006) *J Biol Chem* 281:2095–2103.
25. Zhao H, Li CC, Pardo J, Chu PC, Liao CX, Huang J, Dong JG, Zhou X, Huang Q, Huang B, *et al.* (2005) *J Immunol* 174:5288–5297.
26. Zhao C, Denison C, Huibregtse JM, Gygi S, Krug RM (2005) *Proc Natl Acad Sci USA* 102:10200–10205.
27. Kumar S, Kao WH, Howley PM (1997) *J Biol Chem* 272:13548–13554.
28. Chin LS, Vavalle JP, Li L (2002) *J Biol Chem* 277:35071–35079.
29. Tanaka K, Suzuki T, Chiba T, Shimura H, Hattori N, Mizuno Y (2001) *J Mol Med* 79:482–494.
30. Niwa J, Ishigaki S, Doyu M, Suzuki T, Tanaka K, Sobue G (2001) *Biochem Biophys Res Commun* 281:706–713.
31. Urano T, Saito T, Tsukui T, Fujita M, Hosoi T, Muramatsu M, Ouchi Y, Inoue S (2002) *Nature* 417:871–875.
32. Moynihan TP, Ardley HC, Nuber U, Rose SA, Jones PF, Markham AF, Scheffner M, Robinson PA (1999) *J Biol Chem* 274:30963–30968.
33. Zhang Y, Gao J, Chung KK, Huang H, Dawson VL, Dawson TM (2000) *Proc Natl Acad Sci USA* 97:13354–13359.
34. Kotaja N, Karvonen U, Janne OA, Palvimo JJ (2002) *Mol Cell Biol* 22:5222–5234.
35. Kato H, Sato S, Yoneyama M, Yamamoto M, Uematsu S, Matsui K, Tsujimura T, Takeda K, Fujita T, Takeuchi O, Akira S (2005) *Immunity* 23:19–28.
36. Dastur A, Beaudenon S, Kelley M, Krug RM, Huibregtse JM (2006) *J Biol Chem* 281:4334–4338.

Journal of General Virology (2007), 88, 3323–3333 DOI 10.1099/vir.0.83056-0

Hepatitis C virus non-structural proteins responsible for suppression of the RIG-I/Cardif-induced interferon response

Megumi Tasaka,[1]† Naoya Sakamoto,[1,2]† Yoshie Itakura,[1,3] Mina Nakagawa,[1,2] Yasuhiro Itsui,[1] Yuko Sekine-Osajima,[1] Yuki Nishimura-Sakurai,[1] Cheng-Hsin Chen,[1] Mitsutoshi Yoneyama,[4] Takashi Fujita,[4] Takaji Wakita,[5] Shinya Maekawa,[3] Nobuyuki Enomoto[3] and Mamoru Watanabe[1]

Correspondence
Naoya Sakamoto
nsakamoto.gast@tmd.ac.jp

[1]Department of Gastroenterology and Hepatology, Tokyo Medical and Dental University, Tokyo, Japan

[2]Department for Hepatitis Control, Tokyo Medical and Dental University, Tokyo, Japan

[3]First Department of Internal Medicine, University of Yamanashi, Yamanashi, Japan

[4]Laboratory of Molecular Genetics, Department of Genetics and Molecular Biology, Institute for Virus Research, Kyoto University, Kyoto, Japan

[5]Department of Virology II, National Institute of Infectious Diseases, Tokyo, Japan

Viral infections activate cellular expression of type I interferons (IFNs). These responses are partly triggered by RIG-I and mediated by Cardif, TBK1, IKKε and IRF-3. This study analysed the mechanisms of dsRNA-induced IFN responses in various cell lines that supported subgenomic hepatitis C virus (HCV) replication. Transfection of dsRNA into Huh7, HeLa and HEK293 cells induced an IFN expression response as shown by IRF-3 dimerization, whilst these responses were abolished in corresponding cell lines that expressed HCV replicons. Similarly, RIG-I-dependent activation of the IFN-stimulated response element (ISRE) was significantly suppressed by cells expressing the HCV replicon and restored in replicon-eliminated cells. Overexpression analyses of individual HCV non-structural proteins revealed that NS4B, as well as NS34A, significantly inhibited RIG-I-triggered ISRE activation. Taken together, HCV replication and protein expression substantially blocked the dsRNA-triggered, RIG-I-mediated IFN expression response and this blockade was partly mediated by HCV NS4B, as well as NS34A. These mechanisms may contribute to the clinical persistence of HCV infection and could constitute a novel antiviral therapeutic target.

Received 4 April 2007
Accepted 27 July 2007

INTRODUCTION

Type I interferon (IFN) plays a central role in eliminating virus, not only following clinical therapeutic application but also as a cellular immune response (Samuel, 2001; Taniguchi & Takaoka, 2002). Hepatitis C virus (HCV) infection is characterized by persistence and replication of the virus in the liver, despite an intact host immune system (Alter, 1997). Indeed, even after administration of the currently most potent IFN reagents, as many as half of the patients are refractory to the treatment and fail to eradicate the virus (Fried *et al.*, 2002). These features have led to speculation that HCV escapes from or attenuates the host antiviral response (Katze *et al.*, 2002).

Cellular antiviral responses are primarily mediated by IFN and IFN-stimulated genes (ISGs), including 2,5-oligoadenylate synthetase, dsRNA-dependent protein kinase R (PKR) and MxA proteins, as well as by as yet uncharacterized genes (Itsui *et al.*, 2006; Stark *et al.*, 1998). A study of experimental chimpanzee HCV infection has shown that various cytokines and chemokines are induced in the liver during the course of acute HCV infection and its clearance, and that a considerable proportion of the genes is induced by type I IFN (Bigger *et al.*, 2001).

Control of expression of ISGs is mediated by binding of type I IFNs to their receptors. Following receptor binding, STAT1 and STAT2 are phosphorylated to form ISGF-3, which translocates to the nucleus and binds the IFN-stimulated response element (ISRE), located in the promoter/enhancer region of ISGs, and activates transcription of ISGs (Samuel,

†These authors contributed equally to this work.

2001; Taniguchi *et al.*, 2001; Taniguchi & Takaoka, 2002). ISRE-dependent gene expression is also mediated by binding of the ISRE by molecules such as IRF-1, IRF-3 and IRF-7 (Kanazawa *et al.*, 2004). IRF-3 is a transducer of virus-mediated signalling and plays a critical role in the induction of cellular antiviral responses (Lin *et al.*, 1998; Sato *et al.*, 2000; Taniguchi *et al.*, 2001; Yoneyama *et al.*, 1998). Transcriptional activation and suppression of IRF-3 are inversely correlated with the level of HCV replication *in vitro* (Yamashiro *et al.*, 2006). Following virus infection, IRF-3 is phosphorylated by two cytoplasmic kinases, TBK1 and IKKε (Fitzgerald *et al.*, 2003; Sharma *et al.*, 2003). The phosphorylated IRF-3 forms a homodimer, translocates to the nucleus and predominantly activates expression of the IFN-β gene and certain ISGs (Doyle *et al.*, 2002; Nakaya *et al.*, 2001; Taniguchi & Takaoka, 2002).

RIG-I is a recently identified cytoplasmic DExD/H box RNA helicase that participates in recognition of virus-related dsRNA as a pathogen-related molecular pattern (Yoneyama *et al.*, 2005). RIG-I contains two caspase-recruitment domains (CARDs) in the N terminus and a DExD/H box RNA helicase in the C terminus. MDA5 has been identified as another CARD-containing DExD/H box RNA helicase (Andrejeva *et al.*, 2004). More recently, an adaptor molecule of RIG-I and MDA5, Cardif (also known as IPS-I, MAVS and VISA), has been identified by four independent groups (Kawai *et al.*, 2005; Meylan *et al.*, 2005; Seth *et al.*, 2005; Xu *et al.*, 2005). On association with dsRNA, RIG-I or MDA5 causes conformational changes and homo-oligomerization, and binds the CARD of Cardif (Saito *et al.*, 2007). Cardif subsequently recruits the kinases TBK1 and IKKε, which catalyse phosphorylation and activation of IRF-3 (Yoneyama *et al.*, 1998).

The IRF-3-mediated IFN-β induction pathway could be a target for viruses to counteract antiviral responses and promote their replication in host cells. Ebola virus, bovine viral diarrhea virus (BVDV) and influenza A virus interfere with the activation of IRF-3 through interactions of their virus-encoded proteins (Basler *et al.*, 2003; Schweizer & Peterhans, 2001; Talon *et al.*, 2000). There are several reports that HCV proteins interact with IFN-mediated antiviral systems. The NS5A and E2 proteins have been reported to interfere with the action of IFN by inhibiting the activity of PKR (He & Katze, 2002). It was reported recently that the HCV NS34A protease blocks virus-induced activation of IRF-3, possibly by proteolytic cleavage of Cardif (Foy *et al.*, 2003; Meylan *et al.*, 2005).

The HCV subgenomic replicon is an *in vitro* model that simulates autonomous cellular replication of HCV genomic RNA (Lohmann *et al.*, 1999). Expression of the HCV replicon can be abolished by treatment with small amounts of type I and type II IFNs (Blight *et al.*, 2000; Frese *et al.*, 2002; Guo *et al.*, 2001), suggesting intact IFN receptor-mediated cellular responses. In contrast, viral expression persists in the absence of the exogenous IFN. Baseline expression levels of ISG were substantially decreased in cells expressing the HCV replicon compared with parental Huh7 cells (Kanazawa *et al.*, 2004). These findings led us to speculate that intracellular virus-induced antiviral responses are attenuated or caused to malfunction by the expression of viral proteins.

In this study, we investigated cell lines that support subgenomic HCV replication and HCV cell culture for the dsRNA-induced cellular IFN expression pathway. Here, we report that RIG-I- and Cardif-mediated IFN gene activation is uniformly attenuated in several replicon-expressing cell lines of different lineages and, more importantly, that the HCV NS4B protein is involved in the suppression of antiviral IFN responses.

METHODS

Plasmids. Plasmids pEF-flagRIG-I and ΔRIG-I expressed full-length and C-terminally truncated RIG-I protein, respectively (Yoneyama *et al.*, 2004). The plasmid pER-flagRIG-IKA (RIG-IKA) has a point mutation in the putative ATP-binding site of the RIG-I helicase domain and was used as a negative control for ΔRIG-I and RIG-I full transfection assays. Expression plasmids for full-length Cardif (Cardif), Cardif CARD (CARD) and CARD-truncated Cardif (ΔCARD) were provided by Dr J. Tschopp (University of Lausanne, Switzerland) (Meylan *et al.*, 2005). Expression plasmids for toll-like receptor 3 (TLR3) and TIR domain-containing adaptor inducing IFN-β (TRIF), the transmembrane receptor of dsRNA and the adaptor molecule of TLR3, respectively, were provided by Dr S. Akira (Osaka University, Japan). Plasmids expressing HCV NS345, NS3, NS34A, NS4A, NS4B, NS5A and NS5B were amplified from HCV pCV-J4-L4S (Yanagi *et al.*, 1997) by PCR and subcloned. The DNA fragments were inserted into the vector pcDNA4/TO/*myc*-His (Invitrogen). Nucleotide sequences were confirmed by sequencing. Plasmids TOPO-NS34A (HCV N), TOPO-NS4B (HCV N) and pcDNA-NS4B (HCV JFH1) expressed Myc-tagged NS34A and NS4B proteins derived from the HCV N (Beard *et al.*, 1999) and HCV JFH1 (Wakita *et al.*, 2005) strains, as indicated. Plasmid pISRE-TA-Luc (Invitrogen) contained five copies of consensus ISRE motifs upstream of the firefly luciferase gene. Plasmid pIFNβ-Fluc was constructed by cloning the human IFN-β promoter region, spanning nt −110 to −36, upstream of the firefly luciferase gene of pGL3 Basic (Promega). Plasmid pcDNA3.1 (Invitrogen) was used as an empty vector for mock transfection. pRL-CMV (Promega), which expressed the *Renilla* luciferase protein, was used for correction of transfection efficiency.

Cell culture. HCV strain JFH1-infected Huh7.5.1, Huh7, Huh7.5.1 (kindly provided by Dr F. Chisari, The Scripps Institute, CA, USA; Zhong *et al.*, 2005), HeLa and HEK293 cells were maintained in Dulbecco's modified minimal essential medium (Sigma) supplemented with 2 mM L-glutamine and 10% fetal calf serum at 37 °C with 5% CO_2. Cells expressing the HCV replicon were cultured in medium containing 100 μg G418 (Wako) ml^{-1}.

HCV replicon constructs and transfected cell lines. An HCV subgenomic replicon plasmid, pHCVIbneo-delS (designated pRep-N), was derived from an HCV clone of strain N, genotype 1b, and pSGR-JFH1 was derived from HCV JFH1, genotype 2a (Guo *et al.*, 2001; Wakita *et al.*, 2005). These replicons were reconstructed by substituting the neomycin phosphotransferase gene with a fusion gene comprising *Renilla* luciferase and neomycin phosphotransferase to construct pRep-Reo-1b and pRep-Reo-2a, respectively (Tanabe *et al.*, 2004; Yokota *et al.*, 2003). RNA was synthesized from the replicons using T7 polymerase (Promega) and transfected into Huh7,

HeLa and HEK293 cells. After culture in the presence of G418, cell lines stably expressing the replicon were established (Huh7/1bReo, Huh7/2aReo, HeLa/2aReo and 293/2aReo). We have previously reported that firefly luciferase activities of Feo-replicon-expressing cells correlate well with HCV NS3, NS4A and NS5A protein expression levels and with the levels of replicon RNA (Yokota *et al.*, 2003).

Transient transfection. Transient DNA transfection was performed using Lipofectamine 2000 (Invitrogen) according to the manufacturer's protocol. ISRE reporter assays were carried out as previously described (Nakagawa et al., 2004). To analyse IFN expression in HCV JFH1 cell cultures, a total of 1×10^5 Huh7.5.1, JFH-1 infected Huh7.5.1 and IFN-treated Huh7.5.1 cells were seeded into 24-well plates the day before transfection. Plasmids pISRE-TA-Luc and ΔRIG-I (200 ng each) were transfected using 1 μl Lipofectamine 2000. RIG-IKA was used as a control. Luciferase assays were performed on day 3 post-transfection.

For further study, 400 ng of each non-structural protein was added to 1×10^4 Huh7 or HEK293 cells that had been seeded into 96-well plates the day before transfection. pISRE-TA-Luc and ΔRIG-I (40 ng each) were transfected using 0.5 μl Lipofectamine 2000. RIG-IKA was used as a control.

Western blotting. Preparation of the cytoplasmic and nuclear fractions of cell lysates was carried out as described previously (Tanabe *et al.*, 2004). Protein (20 μg) was separated using NuPAGE 4–12 % Bis/Tris gels (Invitrogen) and blotted onto an Immobilon PVDF membrane (Roche). The membrane was immunoblotted with anti-IRF-3 (Santa Cruz) and detected by chemiluminescence (BM Chemiluminescence Blotting Substrate; Roche).

RT-PCR. Interleukin (IL)-8 mRNA was detected by RT-PCR as described previously (Itsui *et al.*, 2006). The primers used were IL8-S (5′-GCACAAACTTTCAGAGACAGCAGAGCACAC-3′) and IL8-AS (5′-CAGAGCTGCAGAAATCAGGAAGGCTGCCAA-3′).

Indirect immunofluorescence assay. Cells seeded onto tissue culture chamber slides were fixed with cold acetone. The cells were incubated with anti-protein disulphide isomerase (PDI) or anti-Myc antibodies and subsequently with Alexa 488- or Alexa 568-labelled secondary antibodies. Cells were mounted with VECTA SHIELD Mounting Medium and DAPI (Vector Laboratories) and visualized by fluorescence microscopy (BZ-8000; Keyence).

Luciferase reporter assays. Luciferase activity was measured using a 1420 Multilabel Counter (ARVO MX; PerkinElmer) using a Bright-Glo Luciferase Assay System (Promega) or a Dual Luciferase Assay System (Promega). Assays were carried out in triplicate and the results expressed as means ± SD.

MTS assay. To evaluate cell viabilities, dimethylthiazol carboxymethoxyphenyl sulfophenyl tetrazolium (MTS) assays were performed using a CellTiter 96 AQueous One Solution Cell Proliferation Assay kit (Promega) according to manufacturer's instructions.

Statistical analyses. Statistical analyses were performed using an unpaired, two-tailed Student's *t*-test. *P* values of less than 0.05 were considered to be statistically significant.

RESULTS

IRF-3 dimer formation is attenuated in cells expressing the HCV replicon

In the HCV replicon-expressing cell lines Huh7/Rep-Reo-2a, Hela/Rep-Reo-2a and 293/Rep-Reo-2a, replicon expression levels corresponded well to internal *Renilla* luciferase activities. Expression of the HCV replicon was suppressed by IFN in a dose-dependent manner (data not shown).

Activation of RIG-I or MDA5 induces phosphorylation and homodimerization of IRF-3. Following transfection of poly(I:C) into Huh7, HeLa or HEK293 cells, IRF-3 dimers were detected (Fig. 1). However, in cells supporting HCV replicons, IRF-3 dimer formation was almost completely abolished. These findings showed that expression of HCV proteins blocked activation of dsRNA-mediated IFN expression and that these effects were consistently found in several cell lines of different origin.

The HCV replicon suppresses RIG-I/Cardif-induced IFN responses

ISRE reporter activities did not increase in naïve Huh7, HeLa or HEK293 cells following transfection of poly(I:C), whilst overexpression of full-length RIG-I increased poly(I:C)-mediated ISRE reporter activity in Huh7 and HEK293 cells (data not shown). In RIG-I-overexpressing Huh7 cells, transduction with an HCV replicon abolished the poly(I:C)-induced ISRE activation, and elimination of the replicon by IFN treatment restored these ISRE responses (Fig. 2a). Consistent results were obtained by overexpression of ΔRIG-I, a constitutively active form. Transfection of ΔRIG-I in Huh7 and HEK293 cells induced ISRE activation, whilst these responses were abolished or significantly suppressed in cell lines expressing HCV replicons and were recovered by eliminating the replicon by IFN treatment (data not shown). Similarly, ISRE activation by overexpression of Cardif, an adaptor molecule of RIG-I, was almost completely blocked in replicon-expressing cells and was recovered by eliminating the replicon from the cells (data not shown). The RIG-I-mediated IFN response was

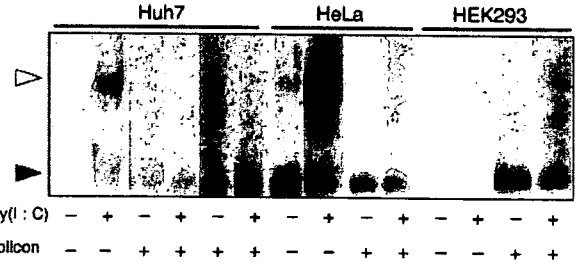

Fig. 1. Double-stranded RNA-induced IRF-3 dimer formation in cell lines that support HCV subgenomic replication. Poly(I:C) was transfected into naïve Huh7, HeLa and HEK293 cells, and into corresponding cell lines expressing the HCV replicon. Six hours after transfection, cell lysates were prepared, separated in polyacrylamide gels and blotted onto PVDF membrane. The membrane was immunoblotted with anti-IRF-3 and visualized by chemiluminescence (see Methods). The positions of the IRF-3 dimer (open arrowhead) and monomer (closed arrowhead) are indicated.

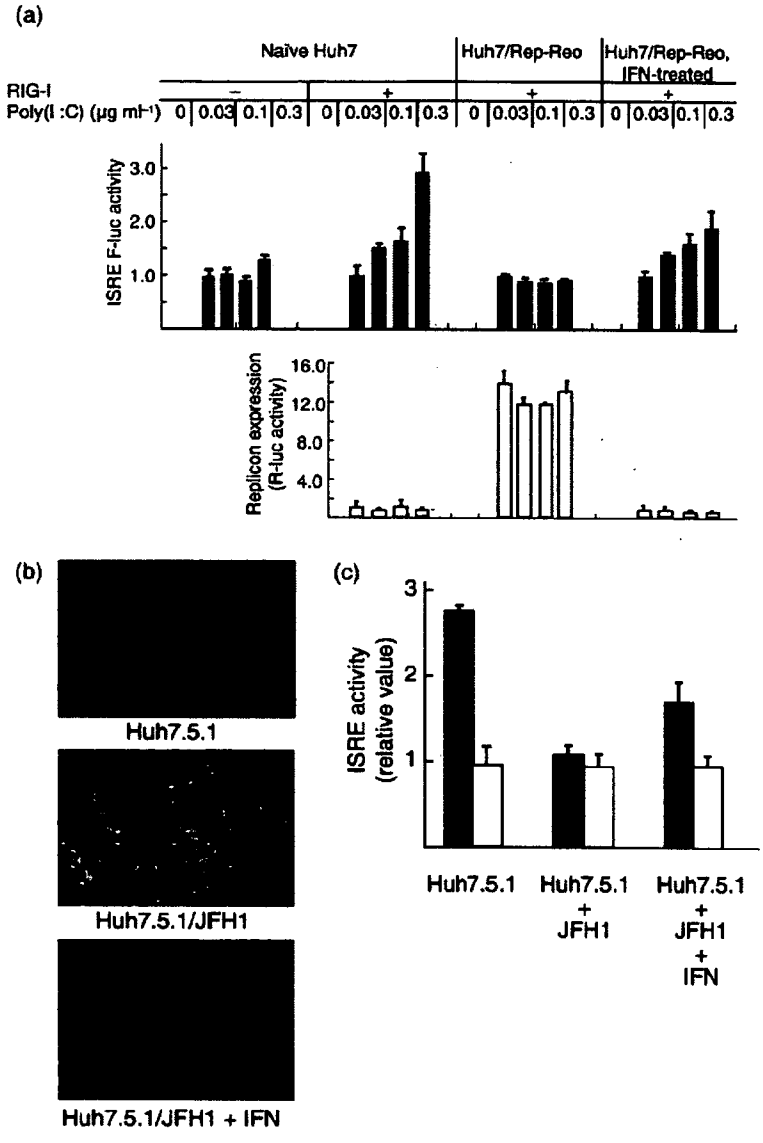

Fig. 2. Suppression of dsRNA-induced, RIG-I-mediated ISRE activation by HCV replication. (a) The HCV replicon suppresses transcriptional activation after poly(I:C) stimulation. The RIG-I expression plasmid and pISRE-TA-Luc were transiently transfected into the cell lines indicated. The following day, the amounts of poly(I:C) indicated were transfected into the corresponding cell lines and dual luciferase assays were carried out 8 h after transfection. Filled bars indicate ISRE-regulated firefly luciferase (F-luc) activities and open bars indicate *Renilla* luciferase (R-luc) activities representing replicon expression levels. In both graphs, scales for the *y*-axis are shown as relative values. Assays were carried out in triplicate and results are shown as means ± SD. (b) Immunofluorescence microscopy results. Huh7.5.1 cells infected with HCV JFH1 (Huh7.5.1/JFH1) and JFH1-infected cells from which the virus had been eliminated by IFN treatment (Huh7.5.1/JFH1+IFN) were incubated with anti-core primary antibodies followed by Alexa Fluor-conjugated secondary antibody (green). Nuclei were stained with DAPI (blue). (c) ISRE activation by ΔRIG-I overexpression. The plasmid pISRE-TA-Luc was co-transfected with ΔRIG-I (filled bars) or RIG-IKA (empty bars) into naïve Huh7.5.1, Huh7.5.1/JFH1 or Huh7.5.1/JFH1+IFN cells. Luciferase assays were carried out 8 h after transfection. The *y*-axis indicates ISRE-regulated luciferase activity shown as relative values. Assays were carried out in triplicate and results are shown as means ± SD.

also suppressed in HCV JFH1 virus cell culture. In JFH1-infected Huh7.5.1 cells, ΔRIG-I-induced ISRE reporter activation was significantly suppressed, but was recovered in IFN-treated, virus-eliminated cells (Fig. 2b and c). These results demonstrated that RIG-I- and Cardif-mediated antiviral responses were substantially suppressed by both subgenomic and genomic viral replication in both hepatocyte- and non-hepatocyte-derived host cells.

NS34A and NS4B are responsible for suppressing RIG-I-mediated IFN responses

We next sought to define which HCV proteins were responsible for inhibition of the RIG-I- and IRF-3-mediated IFN induction pathway. We constructed expression plasmids that expressed the non-structural proteins NS345, NS3, NS34A, NS4A, NS4B, NS5A and NS5B (Fig. 3a). We transfected each expression plasmid with simultaneous activation of the RIG-I pathway by overexpression of ΔRIG-I, Cardif, TBK1 and IKKε (Fig. 3b–e). Expression of full-length non-structural (NS345) and NS34A proteins inhibited ISRE activation mediated by expression of RIG-I and Cardif but not that mediated by TBK1 and IKKε. Interestingly, it was found that NS4B also inhibited ISRE activation mediated by expression of RIG-I and Cardif, but not by TBK1 and IKKε. Consistent with Fig. 3(b), overexpression of NS4B significantly suppressed ΔRIG-I-induced activation of the authentic IFN-β promoter (Fig. 3f).

Another group has studied IFN antagonism of flavivirus non-structural proteins and has reported that HCV NS4B did not affect IFN responses (Muñoz-Jordán *et al.*, 2005).

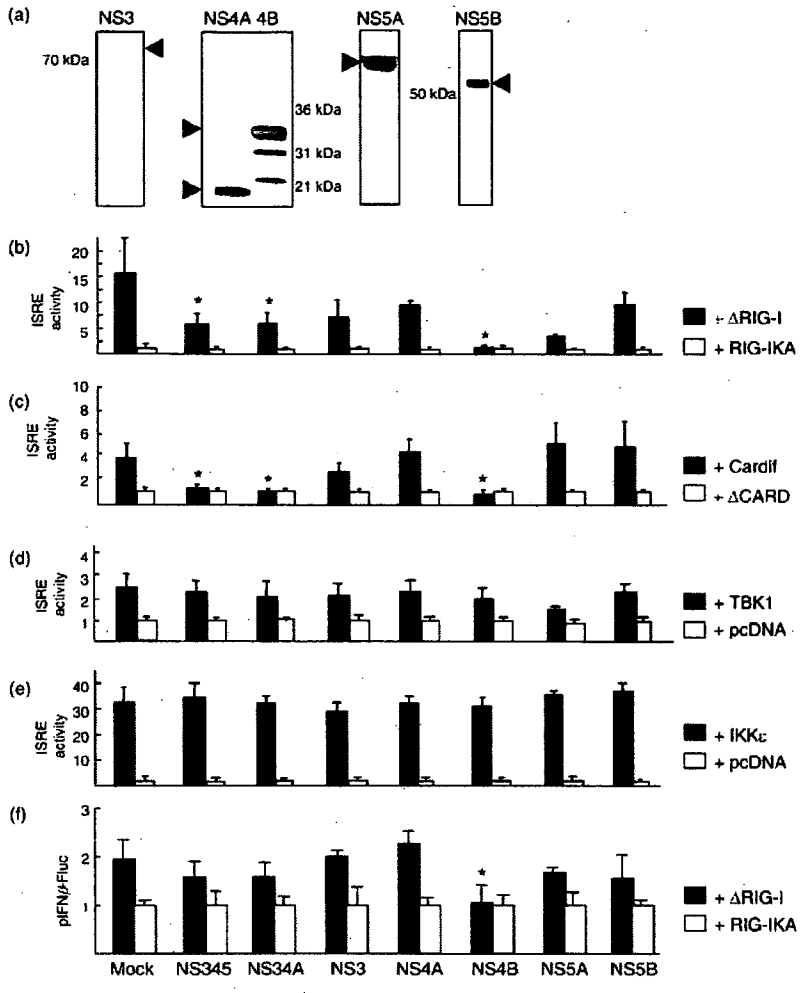

Fig. 3. Co-transfection analyses using plasmids that express individual HCV non-structural proteins. (a) Western blotting. Plasmids expressing the indicated Myc-tagged HCV proteins were transfected into Huh7 cells. Western blotting was carried out using anti-Myc antibody. (b–e) The following plasmids were co-transfected into Huh7 cells: pISRE-TA-Luc, pRL-CMV, the indicated plasmids expressing ΔRIG-I (b), Cardif (c), TBK1 (d) and IKKε (e), and the indicated plasmids expressing individual HCV non-structural proteins. Plasmids RIG-IKA, ΔCARD or pcDNA were used as negative controls as indicated. Twenty-four hours after transfection, luciferase activities were measured. The *y*-axis shows relative values. Assays were carried out in triplicate and results are given as means ± SD. *, $P<0.05$. (f) pIFN-β and pRL-CMV were co-transfected into Huh7 cells, with plasmids expressing individual HCV non-structural proteins and plasmid expressing ΔRIG-I. Luciferase activities were measured 24 h after transfection. The *y*-axis shows relative values. Assays were carried out in triplicate and results are given as means ± SD. *, $P<0.05$. Plasmid RIG-IKA was used as a negative control.

To investigate strain-specific differences in the characteristics of NS4B proteins, we performed co-transfection assays using NS4B expression constructs from HCV N (Beard *et al.*, 1999) and JFH1 (Wakita *et al.*, 2005) strains, as well as HCV strain J4 (Fig. 4a and b). All NS4B constructs suppressed ΔRIG-I- or Cardif-mediated ISRE activation. These results suggested that the above-described effects of NS4B were independent of HCV strain.

NS4B has been reported to induce an unfolded protein response or endoplasmic reticulum (ER) stress through ATF6 or IRE1-X box protein (XBP1) pathways (Zheng *et al.*, 2005). The ER stress induces production of IL-8, which has been reported to interfere with the IFN system (Polyak *et al.*, 2001). Therefore, we detected expression of IL-8 using RT-PCR in cells with and without overexpression of NS4B. As shown in Fig. 4(c), no significant difference was observed in IL-8 mRNA levels among mock-, NS34A- and NS4B-transfected cells. These results showed that NS4B overexpression in the present study did not induce expression of IL-8 and that the IFN-antagonizing effects of NS4B were independent of IL-8.

It has been reported that NS34A suppresses the TLR3-mediated IFN response (Breiman *et al.*, 2005; Ferreon *et al.*, 2005). However, overexpression of HCV non-structural proteins did not suppress ISRE activation that was induced by overexpression of TLR-3 or TRIF (Fig. 5a and b), nor did NS34A from two different HCV strains, J4 and N, show significant suppression of TRIF-mediated ISRE activation (Fig. 5c). Although strain-specific differences might be involved, these data suggest that neither NS34A nor NS4B affect the TLR3-triggered, TRIF-mediated IFN expression signalling pathway.

The NS4B N terminus is involved in inhibition of the RIG-I-mediated pathway

Given the result that NS4B suppressed the RIG-I-mediated IFN expression pathway, we next investigated which domain of NS4B was responsible. We constructed plasmids that expressed truncated NS4B in which the protein-coding frame was truncated at four positions corresponding to the five transmembrane domains (Lundin *et al.*, 2003) (Fig. 6a).

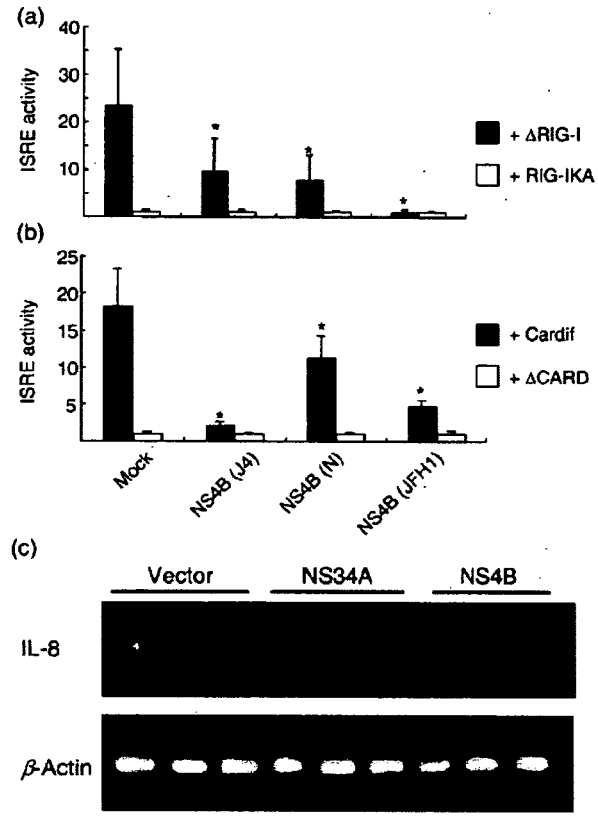

Fig. 4. Co-transfection analyses of HCV NS4B proteins of different origins. NS4B (J4), NS4B (N) and NS4B (JFH1) denote HCV NS4B proteins that were cloned from HCV strains J4, N and JFH1, respectively. The NS4B plasmids indicated were co-transfected with plasmids expressing ΔRIG-I (a) or Cardif (b). Luciferase activities were measured 24 h after transfection. The *y*-axis shows relative values. Assays were carried out in triplicate and results are given as means ± SD. *, $P<0.05$. (c) Semi-quantitative detection of IL-8 mRNA by RT-PCR. cDNA was prepared from Huh7 cells transfected with empty vector or with NS34A or NS4B expression plasmid.

Expression and subcellular localization of NS4B truncated proteins were visualized by indirect immunofluorescence assays (Fig. 7). Each of the NS4B truncated proteins was localized predominantly to the perinuclear rim as dense spots. Some of the spots were similar to the staining of the ER-resident host protein PDI, consistent with previous reports (Lindström *et al.*, 2006; Lundin *et al.*, 2006). These truncated expression plasmids were co-transfected with Cardif expression plasmids into Huh7 cells. As shown in Fig. 6(b), Cardif-mediated ISRE activation was significantly suppressed by co-transfection of NS4Bt1–156 and NS4Bt1–186, as well as full-length NS4B, whilst transfection of NS4Bt90–260 and NS4Bt110–260 did not significantly suppress Cardif-mediated ISRE activation. The shortest construct, NS4Bt131–260, partially retained the ability to reduce ISRE activity. These results suggested that the N-terminal domain of NS4B, which includes aa 1–110, might function directly to suppress RIG-I-mediated IFN expression responses.

DISCUSSION

The recent discovery of cytoplasmic dsRNA sensor molecules has resulted in rapid expansion of knowledge about the IFN-mediated virus defence pathway (Yoneyama *et al.*, 2004). Several reports suggest that viruses target the IFN system to establish replication in the host cells (Kato *et al.*, 2006). We have confirmed that the dsRNA-triggered, IRF-3-mediated IFN activation pathway was blocked in several replicon-supporting cell lines (Fig. 1). Similarly, the dsRNA responses were substantially suppressed in HCV JFH-1 cell culture compared with parental Huh7 cells (Fig. 2b and c). Overexpression analyses showed that RIG-I- and Cardif-mediated ISRE activation was significantly suppressed in HCV replicon-expressing cells, which recovered after elimination of the replicon by IFN treatment (Fig. 2a). In contrast, TBK1- or IKKε-mediated ISRE activation was not suppressed in replicon-expressing cells. Overexpression of individual HCV non-structural proteins revealed that not only NS34A but also NS4B inhibited the ISRE activation signal (Figs 3, 4 and 5). These results suggested that HCV non-structural proteins suppress the IFN induction pathway and that the target host molecule could be Cardif or an unknown adaptor molecule acting between Cardif and TBK1/IKKε.

NS4B protein is a 27 kDa hydrophobic integral membrane protein that is localized in the ER with other non-structural proteins. Studies on other flaviviruses such as Kunjin virus and BVDV support the notion that NS4B may indeed be an essential part of the replication mechanism (Grassmann *et al.*, 2001; Khromykh *et al.*, 2000; Li & McNally, 2001; Qu *et al.*, 2001). These systems have demonstrated that intact NS4B is necessary in a *cis* configuration in the polyprotein for maintaining viral replication (Grassmann *et al.*, 2001; Khromykh *et al.*, 2000). Furthermore, single mutations in NS4B alter the cytopathic effects of BVDV and even mediate changes in the cellular tropism of Dengue virus (Hanley *et al.*, 2003; Qu *et al.*, 2001). In HCV, the search for cell-culture-adaptive mutations in HCV subgenomic replicons has led to the generation of mutations in the NS4B region that confer higher replication levels and resistance to IFNs, as well as broadening the tropism for different cell lines (Lohmann *et al.*, 2003; Sumpter *et al.*, 2004; Zhu *et al.*, 2003). These pieces of evidence may imply that NS4B is not only part of the replication machinery but may also have other functions that enable establishment of viral replication.

NS4B truncation assays showed that RIG-I/Cardif-mediated ISRE activation was significantly suppressed by expression of N terminus-containing constructs (Fig. 6). These results imply that the N-terminal domain of NS4B, which is located between positions 1 and 110, may be essential for suppressing IFN expression responses in host

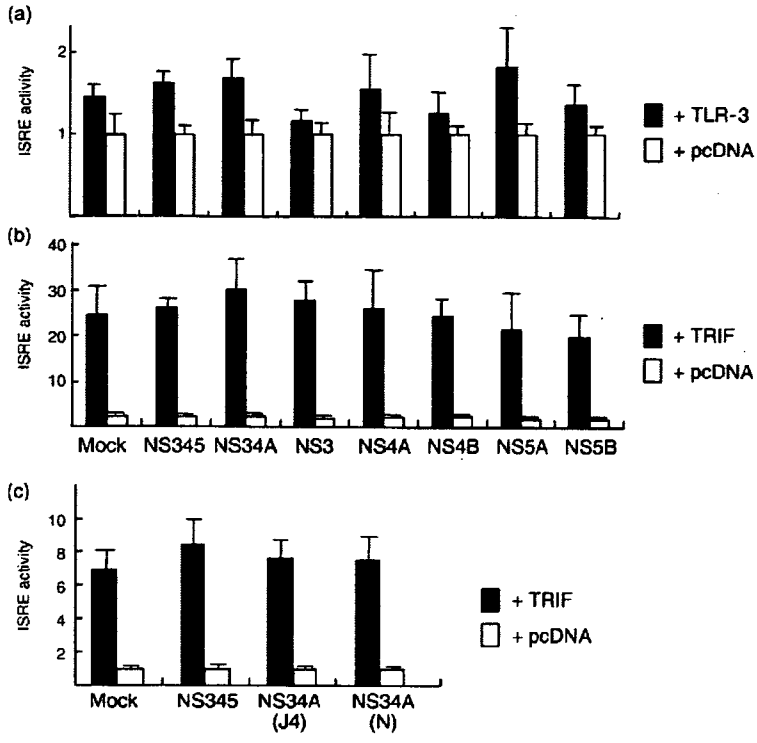

Fig. 5. Co-transfection analyses of HCV non-structural proteins and plasmid expressing TLR-3 or TRIF. (a, b). The following plasmids were co-transfected into Huh7 cells: pISRE-TA-Luc, pRL-CMV, plasmids expressing TLR-3 or TRIF and plasmids expressing individual HCV non-structural proteins, as indicated. Luciferase activities were measured 24 h after transfection. The *y*-axis shows relative values. Assays were carried out in triplicate and results are given as means ± SD. (c) NS34A (J4) and NS34A (N) denote plasmids expressing HCV NS34A derived from HCV strains J4 and N, respectively. The NS4B plasmids indicated were co-transfected with pISRE-TA-Luc, pRL-CMV and plasmids expressing TRIF or pcDNA. Luciferase activities were measured 24 h after transfection. The *y*-axis shows relative values. Assays were carried out in triplicate and results are given as means ± SD.

cells. Lindström *et al.*, (2006) investigated single point mutations in NS4B that negatively affected expression efficiency of the HCV replicon and reported that most of the active mutations were located around the N-terminal domain. A distinctive feature of NS4B is that it requires membrane rearrangement to form its native structure

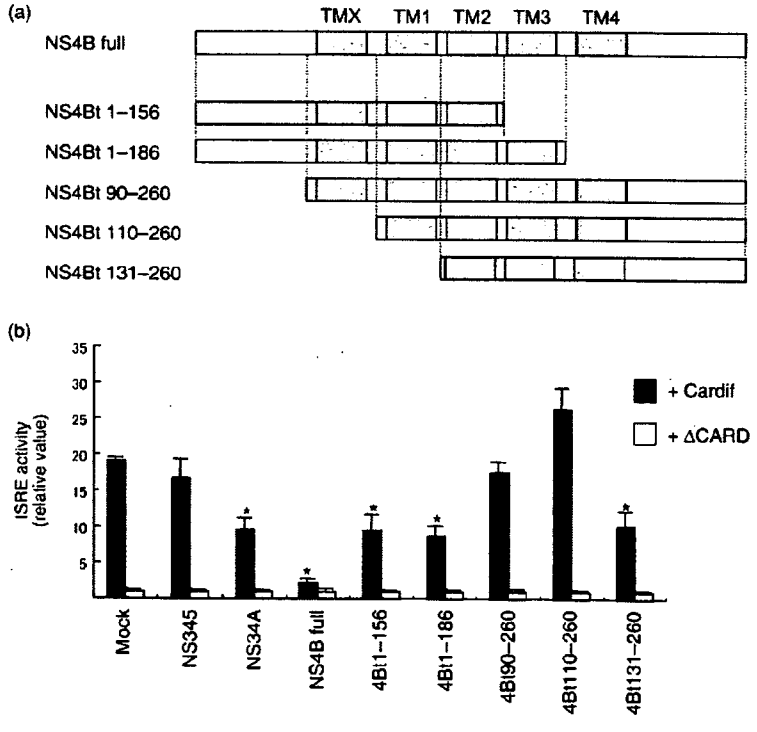

Fig. 6. Co-transfection analyses using truncated NS4B expression constructs. (a) Truncated constructs of NS4B. The protein-coding frame of NS4B was truncated in five constructs corresponding to the five transmembrane domains, as reported by Lundin *et al.* (2003). (b) The truncated NS4B plasmids, pISRE-TA-Luc and the Cardif- or ΔCARD-expressing plasmids indicated were co-transfected into Huh7 cells. Luciferase activities were measured 24 h after transfection. Results are given as means ± SD.

(Lindström *et al.*, 2006; Lundin *et al.*, 2006). The HCV polyprotein is translated from a single reading frame and subjected to proteolytic cleavage by the host signal peptidase and two viral proteases (Grakoui *et al.*, 1993). The mature form of NS4B is localized in the ER and constitutes a subcellular structure called the membrane-associated focus (MAF) (Gretton *et al.*, 2005). Once the NS4B is cleaved, the N-terminal peptide of NS4B is translocated from the cytoplasmic to the luminal side, giving it a fifth transmembrane region (Lundin *et al.*, 2006). The N-terminal amphipathic helix (AH) 1 of NS4B is necessary for this translocation and for MAF formation; NS4B molecules that were truncated at the AH1 lacked the ability to create the MAF, to translocate and to replicate (Elazar *et al.*, 2004; Lindström *et al.*, 2006).

In our assay, NS4Bt131–260 regained the ability to reduce ISRE activity. As we confirmed that all mutants co-localized with the ER, there may be some effect of the N-terminal localization of this mutant. The precise mechanism of NS4B suppression is still not clear and further experiments are needed.

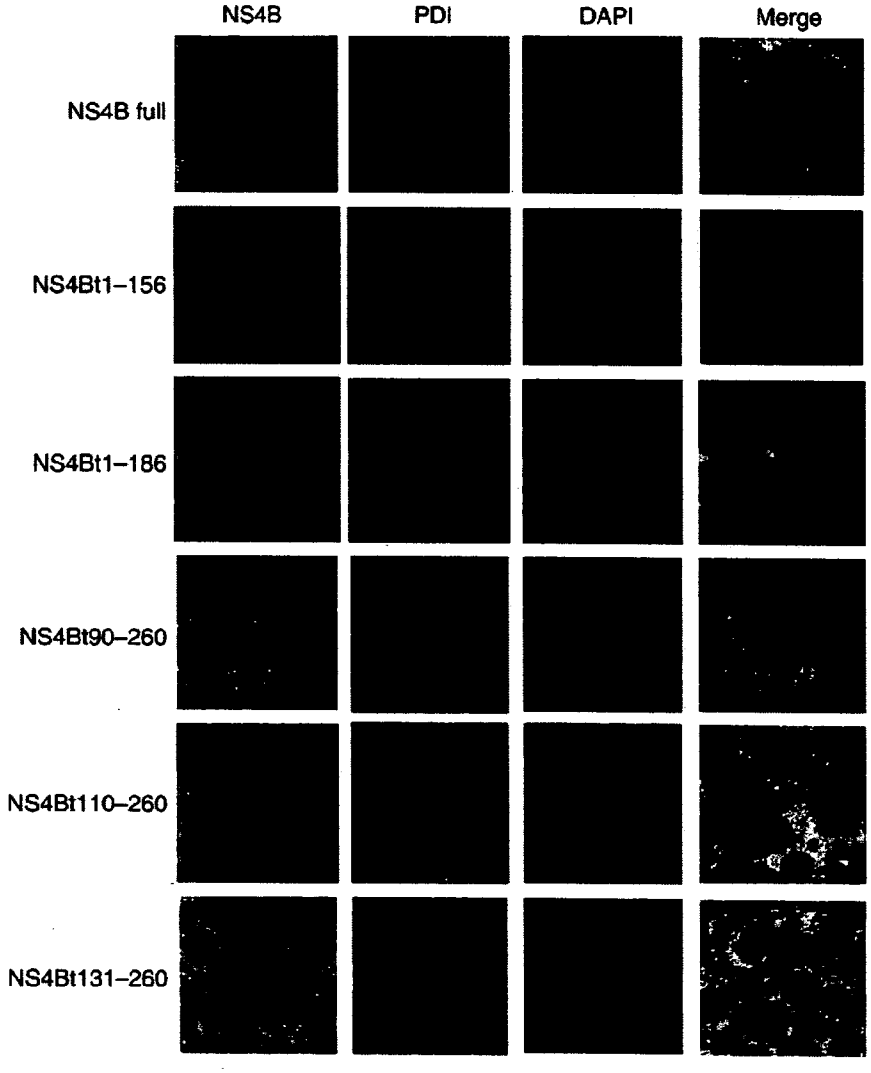

Fig. 7. Indirect immunofluorescence analysis of truncated NS4B proteins. The NS4B constructs indicated were transiently transfected into Huh7 cells. After 48 h, cells were labelled with anti-Myc or anti-PDI antibody. NS4B proteins were immunostained with Alexa Fluor 488-labelled goat anti-mouse IgG, whilst PDI was stained with Alexa Fluor 568-labelled goat anti-rabbit IgG. DAPI staining revealed the nuclear chromatin. Representative immunofluorescence images derived from a number of experiments are shown as four images of a single focal plane of Huh7 cells, showing NS4B proteins (green), PDI (red), DAPI staining (blue) and the superimposed images (merge).

NS4B has been reported to induce an unfolded protein response or ER stress (Zheng *et al.*, 2005). Accumulation of unfolded or misfolded proteins in the ER is detected by three ER sensor proteins, ATF6, IRE-1 and PKR-like ER kinase (PERK), and triggers the unfolded protein response as a stress response and induces expression of molecular chaperon proteins, global shut-off of protein translation and apoptotic cell death (Mori, 2000). Therefore, it may be possible that transgenic overexpression of NS4B induces ER stress and suppresses overall protein synthesis, including that of IFNs. In our experiments, however, NS4B suppressed the ISRE-mediated IFN gene activation but did not suppress non-specific protein expression, as demonstrated by *Renilla* luciferase activity in the control plasmid driven by the herpes simplex thymidine kinase promoter. In addition, the growth and viability of cells that overexpressed NS4B did not differ from untransfected cells or from those transfected with the other HCV proteins. IL-8 overproduction induced by ER stress was not observed in our NS4B-overexpressing cells (Fig. 4c). These findings indicated that the inhibitory effect of NS4B is specific to the IFN induction pathway and is not a non-specific effect through ER stress.

In conclusion, we have shown that dsRNA-induced IFN expression was suppressed by NS4B. These virus–host interactions probably contribute to HCV persistence and to the pathogenesis of HCV-associated liver disease.

ACKNOWLEDGEMENTS

We are indebted to Dr Jürg Tschopp for providing Cardif, ΔCARD and CARD, and to Dr Frank Chisari for providing the Huh7.5.1 cell line. This study was supported by grants from the Japan Society for the Promotion of Science, Miyakawa Memorial Research Foundation and Viral Hepatitis Research Foundation of Japan.

REFERENCES

Alter, M. J. (1997). Epidemiology of hepatitis C. *Hepatology* **26**, 62S–65S.

Andrejeva, J., Childs, K. S., Young, D. F., Carlos, T. S., Stock, N., Goodbourn, S. & Randall, R. E. (2004). The V proteins of paramyxoviruses bind the IFN-inducible RNA helicase, mda-5, and inhibit its activation of the *IFN-β* promoter. *Proc Natl Acad Sci U S A* **101**, 17264–17269.

Basler, C. F., Mikulasova, A., Martinez-Sobrido, L., Paragas, J., Muhlberger, E., Bray, M., Klenk, H. D., Palese, P. & Garcia-Sastre, A. (2003). The Ebola virus VP35 protein inhibits activation of interferon regulatory factor 3. *J Virol* **77**, 7945–7956.

Beard, M. R., Abell, G., Honda, M., Carroll, A., Gartland, M., Clarke, B., Suzuki, K., Lanford, R., Sangar, D. V. & Lemon, S. M. (1999). An infectious molecular clone of a Japanese genotype 1b hepatitis C virus. *Hepatology* **30**, 316–324.

Bigger, C. B., Brasky, K. M. & Lanford, R. E. (2001). DNA microarray analysis of chimpanzee liver during acute resolving hepatitis C virus infection. *J Virol* **75**, 7059–7066.

Blight, K. J., Kolykhalov, A. A. & Rice, C. M. (2000). Efficient initiation of HCV RNA replication in cell culture. *Science* **290**, 1972–1974.

Breiman, A., Grandvaux, N., Lin, R., Ottone, C., Akira, S., Yoneyama, M., Fujita, T., Hiscott, J. & Meurs, E. F. (2005). Inhibition of RIG-I-dependent signaling to the interferon pathway during hepatitis C virus expression and restoration of signaling by IKKε. *J Virol* **79**, 3969–3978.

Doyle, S., Vaidya, S., O'Connell, R., Dadgostar, H., Dempsey, P., Wu, T., Rao, G., Sun, R., Haberland, M. & other authors (2002). IRF3 mediates a TLR3/TLR4-specific antiviral gene program. *Immunity* **17**, 251–263.

Elazar, M., Liu, P., Rice, C. M. & Glenn, J. S. (2004). An N-terminal amphipathic helix in hepatitis C virus (HCV) NS4B mediates membrane association, correct localization of replication complex proteins, and HCV RNA replication. *J Virol* **78**, 11393–11400.

Ferreon, J. C., Ferreon, A. C., Li, K. & Lemon, S. M. (2005). Molecular determinants of TRIF proteolysis mediated by the hepatitis C virus NS3/4A protease. *J Biol Chem* **280**, 20483–20492.

Fitzgerald, K. A., McWhirter, S. M., Faia, K. L., Rowe, D. C., Latz, E., Golenbock, D. T., Coyle, A. J., Liao, S. M. & Maniatis, T. (2003). IKKε and TBK1 are essential components of the IRF3 signaling pathway. *Nat Immunol* **4**, 491–496.

Foy, E., Li, K., Wang, C., Sumpter, R., Jr, Ikeda, M., Lemon, S. M. & Gale, M., Jr (2003). Regulation of interferon regulatory factor-3 by the hepatitis C virus serine protease. *Science* **300**, 1145–1148.

Frese, M., Schwärzle, V., Barth, K., Krieger, N., Lohmann, V., Mihm, S., Haller, O. & Bartenschlager, R. (2002). Interferon-γ inhibits replication of subgenomic and genomic hepatitis C virus RNAs. *Hepatology* **35**, 694–703.

Fried, M. W., Shiffman, M. L., Reddy, K. R., Smith, C., Marionos, G., Goncales, F. L., Häussinger, D., Diago, M., Garosi, G. & other authors (2002). Peginterferon α-2a plus ribavirin for chronic hepatitis C virus infection. *N Engl J Med* **347**, 975–982.

Grakoui, A., Wychowski, C., Lin, C., Feinstone, S. M. & Rice, C. M. (1993). Expression and identification of hepatitis C virus polyprotein cleavage products. *J Virol* **67**, 1385–1395.

Grassmann, C. W., Isken, O., Tautz, N. & Behrens, S. E. (2001). Genetic analysis of the pestivirus nonstructural coding region: defects in the NS5A unit can be complemented in *trans*. *J Virol* **75**, 7791–7802.

Gretton, S. N., Taylor, A. I. & McLauchlan, J. (2005). Mobility of the hepatitis C virus NS4B protein on the endoplasmic reticulum membrane and membrane-associated foci. *J Gen Virol* **86**, 1415–1421.

Guo, J. T., Bichko, V. V. & Seeger, C. (2001). Effect of alpha interferon on the hepatitis C virus replicon. *J Virol* **75**, 8516–8523.

Hanley, K. A., Manlucu, L. R., Gilmore, L. E., Blaney, J. E., Jr, Hanson, C. T., Murphy, B. R. & Whitehead, S. S. (2003). A trade-off in replication in mosquito versus mammalian systems conferred by a point mutation in the NS4B protein of dengue virus type 4. *Virology* **312**, 222–232.

He, Y. & Katze, M. G. (2002). To interfere and to anti-interfere: the interplay between hepatitis C virus and interferon. *Viral Immunol* **15**, 95–119.

Itsui, Y., Sakamoto, N., Kurosaki, M., Kanazawa, N., Tanabe, Y., Koyama, T., Takeda, Y., Nakagawa, M., Kakinuma, S. & other authors (2006). Expressional screening of interferon-stimulated genes for antiviral activity against hepatitis C virus replication. *J Viral Hepat* **13**, 690–700.

Kanazawa, N., Kurosaki, M., Sakamoto, N., Enomoto, N., Itsui, Y., Yamashiro, T., Tanabe, Y., Maekawa, S., Nakagawa, M. & other authors (2004). Regulation of hepatitis C virus replication by interferon regulatory factor 1. *J Virol* **78**, 9713–9720.

Kato, H., Takeuchi, O., Sato, S., Yoneyama, M., Yamamoto, M., Matsui, K., Uematsu, S., Jung, A., Kawai, T. & other authors (2006). Differential roles of MDA5 and RIG-I helicases in the recognition of RNA viruses. *Nature* **441**, 101–105.

Katze, M. G., He, Y. & Gale, M. (2002). Viruses and interferon: a fight for supremacy. *Nature Reviews* **2**, 675–687.

Kawai, T., Takahashi, K., Sato, S., Coban, C., Kumar, H., Kato, H., Ishii, K. J., Takeuchi, O. & Akira, S. (2005). IPS-1, an adaptor triggering RIG-I- and Mda5-mediated type I interferon induction. *Nat Immunol* **6**, 981–988.

Khromykh, A. A., Sedlak, P. L. & Westaway, E. G. (2000). *cis*- and *trans*-acting elements in flavivirus RNA replication. *J Virol* **74**, 3253–3263.

Li, Y. & McNally, J. (2001). Characterization of RNA synthesis and translation of bovine viral diarrhea virus (BVDV). *Virus Genes* **23**, 149–155.

Lin, R., Heylbroeck, C., Pitha, P. M. & Hiscott, J. (1998). Virus-dependent phosphorylation of the IRF-3 transcription factor regulates nuclear translocation, transactivation potential, and proteasome-mediated degradation. *Mol Cell Biol* **18**, 2986–2996.

Lindström, H., Lundin, M., Häggström, S. & Persson, M. A. (2006). Mutations of the hepatitis C virus protein NS4B on either side of the ER membrane affect the efficiency of subgenomic replicons. *Virus Res* **121**, 169–178.

Lohmann, V., Körner, F., Koch, J., Herian, U., Theilmann, L. & Bartenschlager, R. (1999). Replication of subgenomic hepatitis C virus RNAs in a hepatoma cell line. *Science* **285**, 110–113.

Lohmann, V., Hoffmann, S., Herian, U., Penin, F. & Bartenschlager, R. (2003). Viral and cellular determinants of hepatitis C virus RNA replication in cell culture. *J Virol* **77**, 3007–3019.

Lundin, M., Monné, M., Widell, A., Von Heijne, G. & Persson, M. A. (2003). Topology of the membrane-associated hepatitis C virus protein NS4B. *J Virol* **77**, 5428–5438.

Lundin, M., Lindström, H., Grönwall, C. & Persson, M. A. (2006). Dual topology of the processed hepatitis C virus protein NS4B is influenced by the NS5A protein. *J Gen Virol* **87**, 3263–3272.

Meylan, E., Curran, J., Hofmann, K., Moradpour, D., Binder, M., Bartenschlager, R. & Tschopp, J. (2005). Cardif is an adaptor protein in the RIG-I antiviral pathway and is targeted by hepatitis C virus. *Nature* **437**, 1167–1172.

Mori, K. (2000). Tripartite management of unfolded proteins in the endoplasmic reticulum. *Cell* **101**, 451–454.

Muñoz-Jordán, J. L., Laurent-Rolle, M., Ashour, J., Martinez-Sobrido, L., Ashok, M., Lipkin, W. I. & Garcia-Sastre, A. (2005). Inhibition of alpha/beta interferon signaling by the NS4B protein of flaviviruses. *J Virol* **79**, 8004–8013.

Nakagawa, M., Sakamoto, N., Enomoto, N., Tanabe, Y., Kanazawa, N., Koyama, T., Kurosaki, M., Maekawa, S., Yamashiro, T. & other authors (2004). Specific inhibition of hepatitis C virus replication by cyclosporin A. *Biochem Biophys Res Commun* **313**, 42–47.

Nakaya, T., Sato, M., Hata, N., Asagiri, M., Suemori, H., Noguchi, S., Tanaka, N. & Taniguchi, T. (2001). Gene induction pathways mediated by distinct IRFs during viral infection. *Biochem Biophys Res Commun* **283**, 1150–1156.

Polyak, S. J., Khabar, K. S., Paschal, D. M., Ezelle, H. J., Duverlie, G., Barber, G. N., Levy, D. E., Mukaida, N. & Gretch, D. R. (2001). Hepatitis C virus nonstructural 5A protein induces interleukin-8, leading to partial inhibition of the interferon-induced antiviral response. *J Virol* **75**, 6095–6106.

Qu, L., McMullan, L. K. & Rice, C. M. (2001). Isolation and characterization of noncytopathic pestivirus mutants reveals a role for nonstructural protein NS4B in viral cytopathogenicity. *J Virol* **75**, 10651–10662.

Saito, T., Hirai, R., Loo, Y. M., Owen, D., Johnson, C. L., Sinha, S. C., Akira, S., Fujita, T. & Gale, M., Jr (2007). Regulation of innate antiviral defenses through a shared repressor domain in RIG-I and LGP2. *Proc Natl Acad Sci U S A* **104**, 582–587.

Samuel, C. E. (2001). Antiviral actions of interferons. *Clin Microbiol Rev* **14**, 778–809 (Table of Contents).

Sato, M., Suemori, H., Hata, N., Asagiri, M., Ogasawara, K., Nakao, K., Nakaya, T., Katsuki, M., Noguchi, S. & other authors (2000). Distinct and essential roles of transcription factors IRF-3 and IRF-7 in response to viruses for IFN-α/β gene induction. *Immunity* **13**, 539–548.

Schweizer, M. & Peterhans, E. (2001). Noncytopathic bovine viral diarrhea virus inhibits double-stranded RNA-induced apoptosis and interferon synthesis. *J Virol* **75**, 4692–4698.

Seth, R. B., Sun, L., Ea, C. K. & Chen, Z. J. (2005). Identification and characterization of MAVS, a mitochondrial antiviral signaling protein that activates NF-κB and IRF 3. *Cell* **122**, 669–682.

Sharma, S., tenOever, B. R., Grandvaux, N., Zhou, G. P., Lin, R. & Hiscott, J. (2003). Triggering the interferon antiviral response through an IKK-related pathway. *Science* **300**, 1148–1151.

Stark, G. R., Kerr, I. M., Williams, B. R., Silverman, R. H. & Schreiber, R. D. (1998). How cells respond to interferons. *Annu Rev Biochem* **67**, 227–264.

Sumpter, R., Jr, Wang, C., Foy, E., Loo, Y. M. & Gale, M., Jr (2004). Viral evolution and interferon resistance of hepatitis C virus RNA replication in a cell culture model. *J Virol* **78**, 11591–11604.

Talon, J., Horvath, C. M., Polley, R., Basler, C. F., Muster, T., Palese, P. & Garcia-Sastre, A. (2000). Activation of interferon regulatory factor 3 is inhibited by the influenza A virus NS1 protein. *J Virol* **74**, 7989–7996.

Tanabe, Y., Sakamoto, N., Enomoto, N., Kurosaki, M., Ueda, E., Maekawa, S., Yamashiro, T., Nakagawa, M., Chen, C. H. & other authors (2004). Synergistic inhibition of intracellular hepatitis C virus replication by combination of ribavirin and interferon-α. *J Infect Dis* **189**, 1129–1139.

Taniguchi, T. & Takaoka, A. (2002). The interferon-α/β system in antiviral responses: a multimodal machinery of gene regulation by the IRF family of transcription factors. *Curr Opin Immunol* **14**, 111–116.

Taniguchi, T., Ogasawara, K., Takaoka, A. & Tanaka, N. (2001). IRF family of transcription factors as regulators of host defense. *Annu Rev Immunol* **19**, 623–655.

Wakita, T., Pietschmann, T., Kato, T., Date, T., Miyamoto, M., Zhao, Z., Murthy, K., Habermann, A., Krausslich, H. G. & other authors (2005). Production of infectious hepatitis C virus in tissue culture from a cloned viral genome. *Nat Med* **11**, 791–796.

Xu, L. G., Wang, Y. Y., Han, K. J., Li, L. Y., Zhai, Z. & Shu, H. B. (2005). VISA is an adapter protein required for virus-triggered IFN-β signaling. *Mol Cell* **19**, 727–740.

Yamashiro, T., Sakamoto, N., Kurosaki, M., Kanazawa, N., Tanabe, Y., Nakagawa, M., Chen, C. H., Itsui, Y., Koyama, T. & other authors (2006). Negative regulation of intracellular hepatitis C virus replication by interferon regulatory factor 3. *J Gastroenterol* **41**, 750–757.

Yanagi, M., Purcell, R. H., Emerson, S. U. & Bukh, J. (1997). Transcripts from a single full-length cDNA clone of hepatitis C virus are infectious when directly transfected into the liver of a chimpanzee. *Proc Natl Acad Sci U S A* **94**, 8738–8743.

Yokota, T., Sakamoto, N., Enomoto, N., Tanabe, Y., Miyagishi, M., Maekawa, S., Yi, L., Kurosaki, M., Taira, K. & other authors (2003). Inhibition of intracellular hepatitis C virus replication by synthetic and vector-derived small interfering RNAs. *EMBO Rep* **4**, 602–608.

Yoneyama, M., Suhara, W., Fukuhara, Y., Fukuda, M., Nishida, E. & Fujita, T. (1998). Direct triggering of the type I interferon system by

virus infection: activation of a transcription factor complex containing IRF-3 and CBP/p300. *EMBO J* **17**, 1087–1095.

Yoneyama, M., Kikuchi, M., Natsukawa, T., Shinobu, N., Imaizumi, T., Miyagishi, M., Taira, K., Akira, S. & Fujita, T. (2004). The RNA helicase RIG-I has an essential function in double-stranded RNA-induced innate antiviral responses. *Nat Immunol* **5**, 730–737.

Yoneyama, M., Kikuchi, M., Matsumoto, K., Imaizumi, T., Miyagishi, M., Taira, K., Foy, E., Loo, Y. M., Gale, M., Jr & other authors (2005). Shared and unique functions of the DExD/H-box helicases RIG-I, MDA5, and LGP2 in antiviral innate immunity. *J Immunol* **175**, 2851–2858.

Zheng, Y., Gao, B., Ye, L., Kong, L., Jing, W., Yang, X., Wu, Z. & Ye, L. (2005). Hepatitis C virus non-structural protein NS4B can modulate an unfolded protein response. *J Microbiol* **43**, 529–536.

Zhong, J., Gastaminza, P., Cheng, G., Kapadia, S., Kato, T., Burton, D. R., Wieland, S. F., Uprichard, S. L., Wakita, T. & Chisari, F. V. (2005). Robust hepatitis C virus infection *in vitro*. *Proc Natl Acad Sci U S A* **102**, 9294–9299.

Zhu, Q., Guo, J. T. & Seeger, C. (2003). Replication of hepatitis C virus subgenomes in nonhepatic epithelial and mouse hepatoma cells. *J Virol* **77**, 9204–9210.

Please cite this article in press as: Takahasi et al., Nonself RNA-Sensing Mechanism of RIG-I Helicase and Activation of Antiviral Immune Responses, Molecular Cell (2008), doi:10.1016/j.molcel.2007.11.028

Molecular Cell
Article

Nonself RNA-Sensing Mechanism of RIG-I Helicase and Activation of Antiviral Immune Responses

Kiyohiro Takahasi,[1,6] Mitsutoshi Yoneyama,[2,3,5,6] Tatsuya Nishihori,[1] Reiko Hirai,[2,3] Hiroyuki Kumeta,[1] Ryo Narita,[2,3] Michael Gale, Jr.,[4] Fuyuhiko Inagaki,[1] and Takashi Fujita[2,3,*]

[1]Department of Structural Biology, Graduate School of Pharmaceutical Sciences, Hokkaido University, Sapporo, Hokkaido, 060-0812, Japan

[2]Laboratory of Molecular Genetics, Institute for Virus Research

[3]Laboratory of Molecular Cell Biology, Graduate School of Biostudies

Kyoto University, Kyoto, 606-8507, Japan

[4]Department of Immunology, University of Washington School of Medicine, 1959 NE Pacific Street, H-578 Health Sciences, Box 357650, Seattle, WA 98195-7650, USA

[5]PRESTO, Japan Science and Technology Agency, 4-1-8 Honcho Kawaguchi, Saitama, 332-0012, Japan

[6]These authors contributed equally to this work.

*Correspondence: tfujita@virus.kyoto-u.ac.jp

DOI 10.1016/j.molcel.2007.11.028

SUMMARY

A DExD/H protein, RIG-I, is critical in innate antiviral responses by sensing viral RNA. Here we show that RIG-I recognizes two distinct viral RNA patterns: double-stranded (ds) and 5′ppp single-stranded (ss) RNA. The binding of RIG-I with dsRNA or 5′ppp ssRNA in the presence of ATP produces a common structure, as suggested by protease digestion. Further analyses demonstrated that the C-terminal domain of RIG-I (CTD) recognizes these RNA patterns and CTD coincides with the autorepression domain. Structural analysis of CTD by NMR spectroscopy in conjunction with mutagenesis revealed that the basic surface of CTD with a characteristic cleft interacts with RIG-I ligands. Our results suggest that the bipartite structure of CTD regulates RIG-I on encountering viral RNA patterns.

INTRODUCTION

Viral infections provoke various host responses, including early innate and subsequent adaptive immune responses. Innate responses are genetically programmed to detect a wide range of viral infections and activate a set of genes encoding humoral factors known as cytokines and chemokines. The most important cytokines in viral infection are type I interferons (IFNs), which are secreted and confer antiviral activity to the host (Joklik, 1991; Samuel, 2001). Moreover, IFN and other cytokines critically contribute to the successful activation of acquired immunity. Genomes of higher eukaryotes encode receptors for detecting pathogen molecules called pathogen-associated molecular patterns (PAMPs). Toll-like receptors (TLRs) detect PAMPs of extracellular origin either at the cell surface or in the endosome (Akira et al., 2006). TLR3, TLR7/8, and TLR9 are receptors for viral polynucleotides and trigger the production of cytokines. Unlike bacteria and fungi, viruses strictly require host cells, in which they replicate; therefore, cytoplasmic receptors to detect viral infection and subsequent replication have been hypothesized to exist since the discovery of the IFN system. Recent screening of an expression cDNA library identified an RNA helicase, RIG-I, as a cytoplasmic receptor for viral replication (Yoneyama and Fujita, 2007; Yoneyama et al., 2004).

RIG-I consists of an N-terminal *c*aspase *r*ecruitment *d*omain (CARD), a domain with the signature of DExD/H box helicase (helicase domain), and a C-terminal repression domain (RD) (Saito et al., 2007; Yoneyama et al., 2004). Functional analyses revealed that the helicase domain and RD are required for detecting viral RNA and the CARD triggers the activation of a downstream signaling cascade, including the activation of transcription factors, NF-κB, interferon regulatory factor (IRF)-3, and IRF-7. RD interacts with the helicase domain (helicase linker region) and CARD. A model is proposed that, in the absence of dsRNA, RIG-I adopts a "closed" conformation but upon binding to dsRNA changes to an "open" structure, exposing the CARD. Human and mouse genomes encode another CARD-containing helicase, termed MDA5, and a structurally related helicase without a CARD, LGP2 (Yoneyama et al., 2005). Studies in knockout mice have revealed that both RIG-I and MDA5 function as cytoplasmic sensors and are physiologically critical for antiviral defense (Gitlin et al., 2006; Kato et al., 2005, 2006). Moreover, RIG-I and MDA5 function differently in the recognition of RNA viruses (Gitlin et al., 2006; Kato et al., 2006).

IFN-inducing compounds have been extensively screened in the past, and it was shown that dsRNA, particularly the synthetic cohomopolymer poly I:C, exhibits comparative activity to viral infections (Joklik, 1991; Samuel, 2001). It has been widely accepted that dsRNA is a viral PAMP because it is normally absent in mammalian cells, due to the absence of RNA-dependent RNA polymerase. Poly I:C not only activates TLR3, but when directly introduced into the cytoplasm, preferentially activates MDA5 (Alexopoulou et al., 2001; Kato et al., 2006). Conversely, dsRNA with a nonbiased sequence, prepared by in vitro transcription and annealing, preferentially activates RIG-I (Kato et al., 2006). Recently, it was discovered that ssRNA with 5′ triphosphate (5′ppp ssRNA) is a ligand for RIG-I (Hornung et al.,

Please cite this article in press as: Takahasi et al., Nonself RNA-Sensing Mechanism of RIG-I Helicase and Activation of Antiviral Immune Responses, Molecular Cell (2008), doi:10.1016/j.molcel.2007.11.028

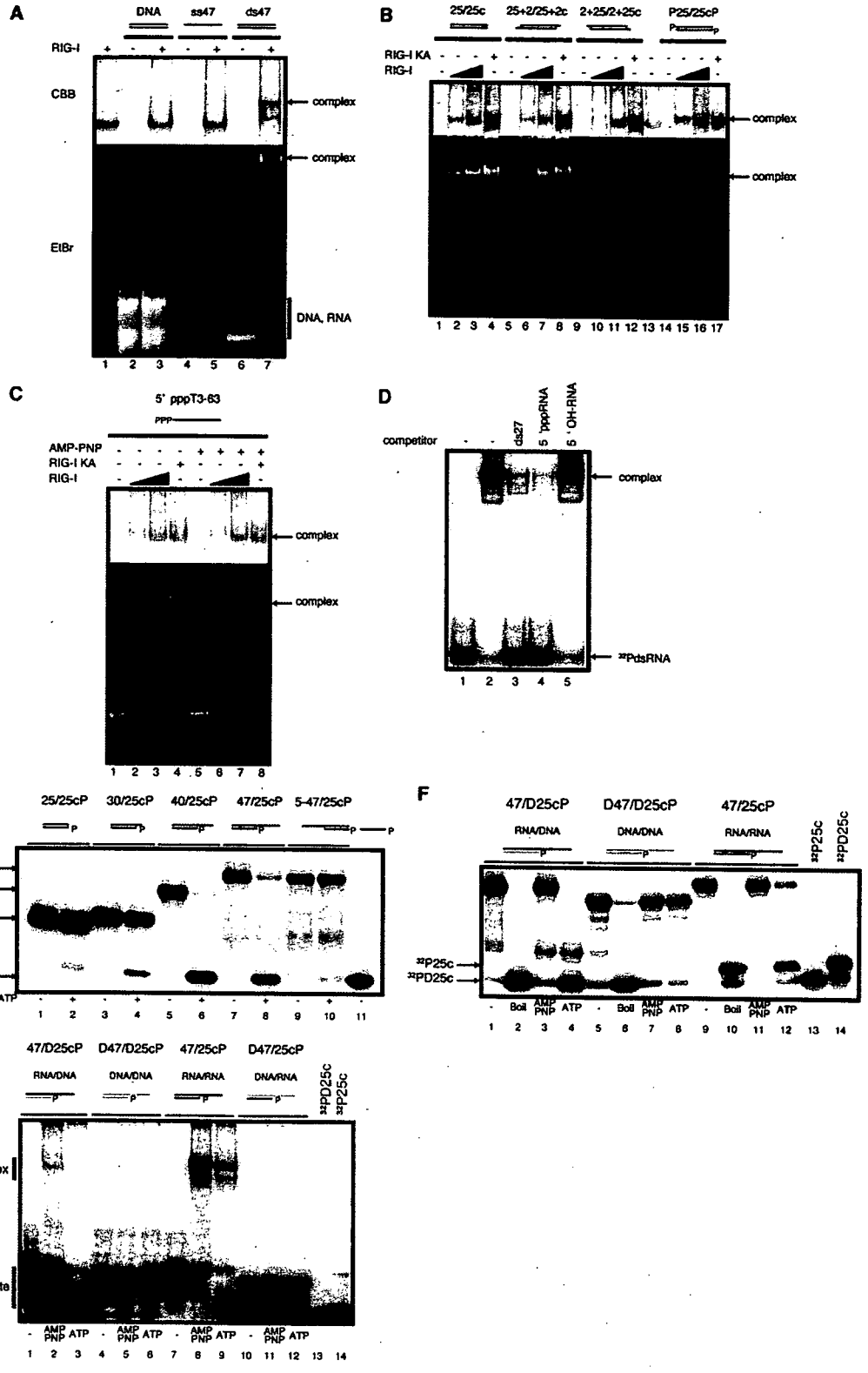

2006; Pichlmair et al., 2006). These observations suggest that RIG-I and MDA5 detect different subtypes of RNA ligands and this reflects virus-specific recognition by these helicases. Thus, it could be defined that dsRNA and 5′ppp ssRNA are recognized by innate immune sensors as "nonself" RNA, whereas "self" RNAs escape from detection due to chemical modification (Fujita, 2006). In this report, biochemical properties, including RNA binding activity, ATPase activity, and helicase activity, of recombinant RIG-I were investigated using various polynucleotides.

RESULTS

Physical Association of RIG-I with Polynucleotides

To investigate the biochemical properties of RIG-I protein, we produced human RIG-I, either the wild-type or a mutant altered in Walker's ATP binding motif (K270A), using a baculovirus system, and purified it to homogeneity. The recombinant proteins were subjected to binding assays with various polynucleotides (Figure S1). The reaction mixtures were separated by nondenaturing PAGE and sequentially stained with ethidium bromide (EtBr) and Coomassie brilliant blue (CBB) to visualize the polynucleotides and RIG-I protein, respectively. RIG-I did not bind to chemically synthesized dsDNA or ssRNA but bound to dsRNA prepared by annealing chemically synthesized complementary RNA strands (Figure 1A), confirming that RIG-I specifically binds to the dsRNA structure (Yoneyama et al., 2004). Because it was reported that dsRNA with a blunt end preferentially activates the RIG-I pathway whereas dsRNA with a 3′ overhang of two nucleotides is preferentially subjected to RNA interference (Marques et al., 2006), oligonucleotides with different end structures including blunt end and 3′ and 5′ overhangs, and oligonucleotides with or without the end phosphate group were tested (Figure 1B). All the dsRNA tested exhibited clear activity to bind the recombinant RIG-I as well as the RIG-I K270A mutant, showing that the structure of the dsRNA, not its end, is critical for physical interaction between RIG-I and dsRNA. Furthermore, the ATP-binding motif of RIG-I is dispensable for binding to dsRNA.

For comparison, 5′ppp ssRNA was similarly tested. We used 63 nucleotide ssRNA (5′pppT3-63) generated in vitro by transcription for binding to RIG-I (Figure 1C). In contrast to chemically synthesized RNA (Figure 1A, lane 5), ssT3-63 exhibited binding to RIG-I, confirming the reports (Hornung et al., 2006; Pichlmair et al., 2006). As reported, ssRNA with 5′ monophosphate failed to bind to RIG-I (Figure S2). This binding is comparable to that of dsRNA and independent of an intact ATP-binding motif (RIG-IK270A) or the presence of an unhydrolyzable ATP analog, AMP-PNP.

To examine the binding sites of dsRNA and 5′ppp ssRNA on RIG-I, a competition experiment was performed (Figure 1D). When recombinant RIG-I was subjected to an electrophoresis mobility shift assay (EMSA) using a radioactive dsRNA probe, a clear complex was detected (lane 2). Complex formation was efficiently inhibited by adding a molar excess of cold dsRNA and 5′ ppp ssRNA but not 5′-OH ssRNA (lanes 3–5), suggesting that the binding sites of dsRNA and 5′ppp ssRNA overlap.

Helicase Activity of RIG-I

RIG-I retains the structural signature of RNA helicases (Cordin et al., 2006). Although previous work demonstrated that a deletion mutant of RIG-I exhibits weak dsRNA unwinding (Marques et al., 2006), helicase activity of the full-length protein has not been shown. We examined the helicase activity of full-length RIG-I in vitro using dsRNA with a different end structure as the substrate (Figure 1E). The blunt-ended dsRNA unwound very inefficiently; however, dsRNA with a 5 nt 3′ overhang significantly unwound and that with a 3′ overhang longer than 15 nt unwound completely. The 3′ overhang is essential, because the 15 nt 5′ overhang is resistant to unwinding. Unwinding requires the hydrolysis of ATP, because AMP-PNP blocked the reaction (Figure 1F, lane 11) and RIG-I K270A is inactive for unwinding (Figure S3). Some RNA helicases act to unwind RNA/DNA duplexes in addition to dsRNA substrates (Rogers et al., 2001). We tested the unwinding of RNA/DNA duplexes and dsDNA. For comparison, substrates with the same nucleotide sequence, including a 3′ overhang, were used (Figure 1F). The dsRNA and RNA/DNA duplexes with a 3′ RNA overhang unwound with comparable efficiency, but the dsDNA was totally resistant. RNA/DNA duplexes with a 3′ DNA overhang did not unwind under the same conditions (our unpublished data). These results are consistent with RIG-I binding to 47/25cP and 47/D25cP but not to D47/D25cP or D47/25cP (Figure 1G). Although the RIG-I/substrate complex is stable in the presence of AMP-PNP, the complex dissociates by the helicase reaction in the presence of ATP (Figure 1G, lanes 2 and 3 and lanes 8 and 9).

Figure 1. RNA-Binding Properties and Helicase Activity of RIG-I

(A) Recombinant RIG-I (30 pmol) was mixed with dsDNA, synthetic 5′OH ssRNA, and dsRNA (50 pmol each) and separated. The gel was stained for nucleic acid (EtBr) and protein (CBB). Under these conditions, EtBr does not stain RIG-I and CBB does not detect oligonucleotides (data not shown).

(B) Twenty-five base pair nucleotides with different end structures (each 10 pmol) were mixed with RIG-I (30 pmol, lanes 2, 6, 10, and 15; 60 pmol, lanes 3, 7, 11, and 16) or mutant K270A (RIG-IKA; 60 pmol, lanes 4, 8, 12, and 17) and resolved by gel electrophoresis as in (A).

(C) RIG-I was mixed with 5′ppp ssRNA in the absence or presence of AMP-PNP and analyzed as in (B). Lanes 2 and 6, 30 pmol RIG-I; lanes 3 and 7, 60 pmol RIG-I; lanes 4 and 8, 60 pmol RIG-IKA.

(D) EMSA using ^{32}P-dsRNA (ds27, 0.08 pmol) as a probe. For binding competition, indicated unlabeled RNAs (500-fold molar excess over the probe) were included.

(E) RNA-unwinding activity of RIG-I. Indicated RNA substrates were analyzed for helicase activity. The reaction was run in the absence (lanes 1, 3, 5, 7, and 9) or presence (lanes 2, 4, 6, 8, and 10) of ATP. Unannealed ^{32}P-p25c was run similarly (lane 11).

(F) RNA/DNA duplex-unwinding activity of RIG-I. Indicated nucleotide duplexes along with dsRNA substrates were analyzed as in (E). Substrate alone, lanes 1, 5, and 9; boiled substrate, lanes 2, 6, and 10; reaction with AMP-PNP, lanes 3, 7, and 11; reaction with ATP, lanes 4, 8, and 12. Unannealed ^{32}P-p25c and pD25c were electrophoresed in lanes 13 and 14, respectively.

(G) EMSA of helicase reaction mixture. Helicase reaction mixtures without competitor RNA were analyzed by native PAGE. Substrate alone, lanes 1, 4, 7, and 10; reaction with AMP-PNP, lanes 2, 5, 8, and 11; reaction with ATP, lanes 3, 6, 9, and 12. Unannealed ^{32}P-p25c and pD25c are electrophoresed in lanes 13 and 14, respectively. Positions of ^{32}P-substrate and RIG-I-substrate complex are indicated.

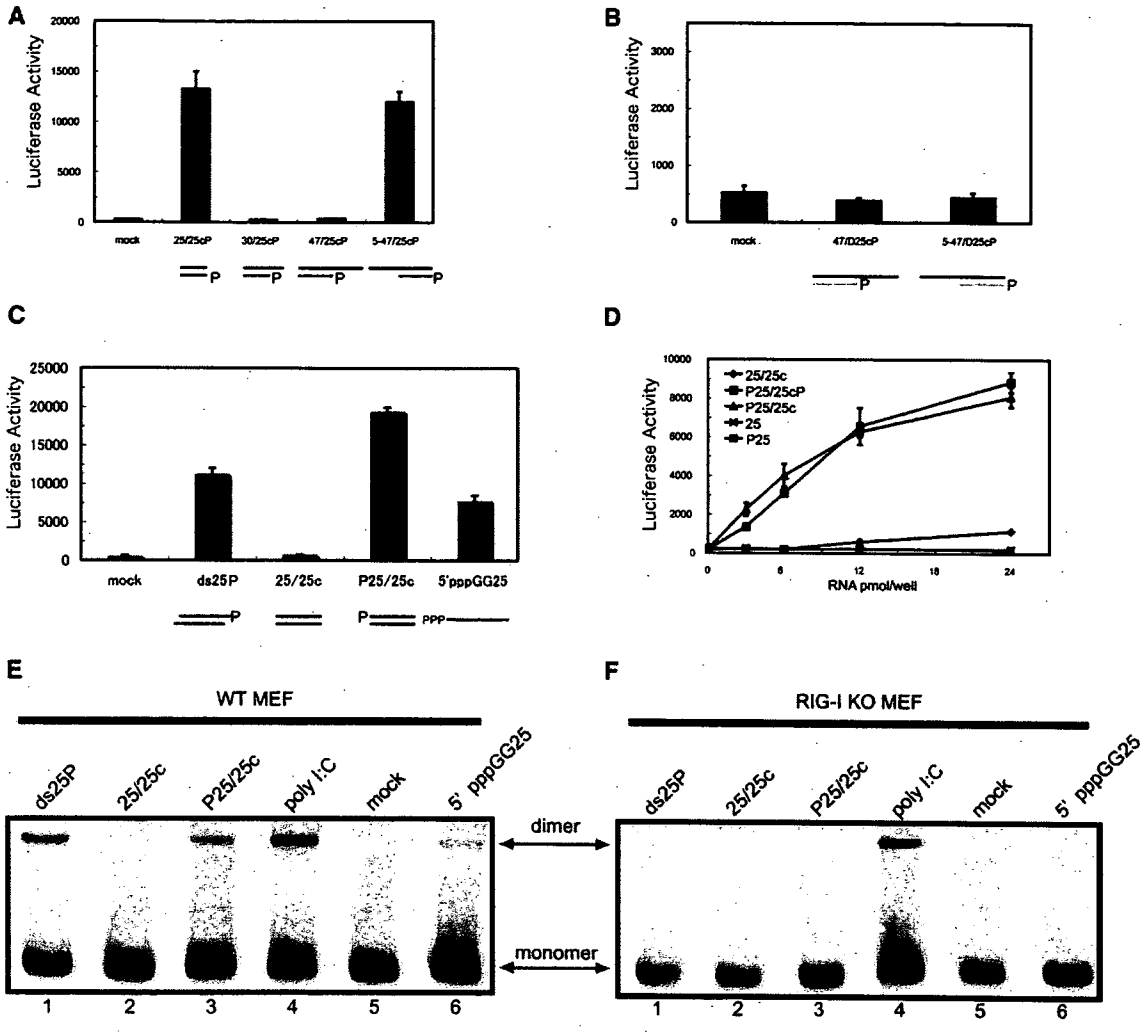

Figure 2. Gene Activation Properties of dsRNA and 5′ppp ssRNA

(A) dsRNA with a 3′ or 5′ overhang was transfected (90 pmol/3 cm dish) into L929/C1B-Luc cells, and luciferase activity derived from an integrated virus-responsive reporter gene was analyzed. RNA/DNA duplexes (B), dsRNAs with various end structures, and 5′ppp ssRNA (C) were similarly analyzed for their potential to activate virus-responsive promoter (30 pmol/well in a 12-well plate). Effect of end phosphorylation on immunogenic activity of dsRNA was analyzed (D). The values are the means ± SD from triplicate experiments. MEFs derived from wild-type mouse (WT MEF) (E) or *RIG-I*$^{-/-}$ mouse (F) in a 3 cm dish were transfected with the indicated RNA (90 pmol) and analyzed for IRF-3 dimerization.

Immunogenic Properties of Various Polynucleotides

The above results reveal the requirement for RIG-I helicase activity to be a 3′ overhang longer than 5 nt. To address the involvement of helicase activity in RIG-I-mediated signaling, we transfected dsRNA used for the helicase assay (Figures 2A and 2B). 30/25cP and 47/25cP, which are highly susceptible to unwinding by RIG-I, did not activate the virus-responsive reporter, p-55C1BLuc, whereas 25/25cP and 5-47/25cP efficiently activated the reporter gene. Likewise, an RNA/DNA duplex, 47/D25cP, which was efficiently unwound by RIG-I, failed to activate the reporter gene. 5-47/D25cP, an RNA/DNA duplex with 5′ RNA overhang, did not activate the reporter, presumably due to its low affinity to RIG-I (Figure S4). These results strongly suggest that helicase activity is reversibly correlated to the immunogenic signal triggered by RIG-I.

On the other hand, ATPase-inducing activity of oligonucleotides is positively correlated to their immunogenic activity. dsRNA and 5′ppp ssRNA, but not 5′-OH ssRNA, induced ATPase activity (Figure S5A); dsRNA with blunt end or 5′ overhang induced ATPase activity, but lower activity was induced by dsRNA with 3′ overhang (Figure S5B). dsRNA is a better ATPase inducer than RNA/DNA duplex (Figure S5C); however, ATPase induction alone may not be sufficient to activate RIG-I for signaling, because 47/25c, a dsRNA with 3′ overhang, induces ATPase significantly (Figure S5B) without signaling (Figure 2A).

Please cite this article in press as: Takahasi et al., Nonself RNA-Sensing Mechanism of RIG-I Helicase and Activation of Antiviral Immune Responses, Molecular Cell (2008), doi:10.1016/j.molcel.2007.11.028

To explore the structural requirement of dsRNA for immunogenic signaling in detail, dsRNA with or without an end phosphate was tested. We found that phosphorylation of one of the strands is sufficient to confer the full activity of dsRNA, whereas ssRNA with a 5′-monophosphate is inactive (Figures 2C and 2D). Because RIG-I strongly binds to dsRNA with or without 5′-monophosphate in vitro (Figure 1B), we investigated the effect of 5′-monophosphate on dsRNA turnover in transfected cells. Figure S6 demonstrates that dsRNA possessing 5′-monophosphate at one of the strands is more stable than 5′-OH dsRNA.

RIG-I Is Required for p-dsRNA- or 5′ppp ssRNA-Induced IRF-3 Activation

To identify which of the sensing molecules is responsible for triggering the signal, p-dsRNA or 5′ppp ssRNA was transfected into wild-type MEFs and MEFs derived from *RIG-I*$^{-/-}$ mice (Figures 2E and 2F). In wild-type MEFs, all the RNA tested, including poly I:C, induced the formation of an IRF-3 dimer; however, in RIG-I-deficient MEFs, only poly I:C activated IRF-3. This result strongly suggests that p-dsRNA and 5′ppp ssRNA triggered signaling through RIG-I, whereas RIG-I is dispensable in the poly I:C-induced activation of IRF-3. The latter observation is consistent with reports that poly I:C is exclusively detected by another sensor, MDA5 (Gitlin et al., 2006; Kato et al., 2006).

dsRNA and 5′ppp ssRNA Induce Similar Conformational Change on RIG-I

The above results suggest that p-dsRNA and 5′ppp ssRNA are specifically sensed by RIG-I; however, poly I:C is distinctly recognized by RIG-I as suggested by the fact that RIG-I binds to poly I:C but is unable to trigger signaling. To explore the events following the physical association of polynucleotides with RIG-I, the complexes were subjected to limited protease digestion to monitor RIG-I conformation. We found that free RIG-I is highly sensitive to trypsin treatment and rapidly degraded (Figure 3A, lanes 1 and 2) (Saito et al., 2007); however, in the presence of dsRNA (25/25c and ds25) or 5′pppGG25, a protease-resistant 30 kDa fragment was generated (Figure 3A) and the process was facilitated in the presence of AMP-PNP (or ATP; our unpublished data). The 5′ppp moiety is critical, as 5′OH-GG25 is inactive. An essentially identical result was obtained by using chymotrypsin, showing that the observation is not due to the specificity of the protease (Figure 3A and Figure S7). These results suggest that, although structurally distinct, p-dsRNA and 5′ppp ssRNA induce similar conformational change of RIG-I upon physical interaction in the presence of AMP-PNP. Sequence analysis and reactivity to a series of monoclonal antibodies to RIG-I revealed that the 30 kDa fragment corresponds to the C-terminal region of RIG-I (our unpublished data). Remarkably, when RIG-I is bound to poly I:C it adopts a distinct conformation, as suggested by the generation of a 66 kDa, but not 30 kDa, fragment (Figure 3B and Figure S7).

RIG-I792–925(CTD) Specifically Recognizes dsRNA and 5′ppp ssRNA, and Interacts with the Helicase Linker Domain

Extensive protease treatment of the RIG-I/dsRNA complex, but not RIG-I alone, yielded a 17 kDa polypeptide (Figure S7). We hypothesized that this fragment was bound to the dsRNA and was protected from digestion. The fragment was further analyzed by mass spectrometry and protein sequencing, revealing that it corresponds to the C-terminal aa 792–925 of RIG-I (our unpublished data). A recombinant RIG-I (792–925, hereafter termed CTD) was subsequently produced in *E. coli*, and its RNA-binding properties were examined. As a control, the helicase domain (194–791), similarly produced in *E. coli*, was also tested. Figure 3C shows that dsRNA bound to RIG-I CTD, albeit with less affinity than full-length RIG-I, but not to the helicase domain. Competition experiments demonstrated that the interaction was specific to dsRNA and 5′ppp ssRNA (Figure 3C, lanes 6–12). This selective binding of RIG-I 792–925 was also demonstrated under different conditions, in which higher concentrations of unlabeled RNA were used (Figure 3D). Because the helicase domain, which catalyzes the unwinding of dsRNA, has been implicated in the binding of dsRNA (Saito et al., 2007), the identification of a distinct domain was a surprise. Furthermore, end monophosphate residue in dsRNA is not required for interaction with CTD and 5′ppp-dsRNA binds to RIG-I better than 5′ppp ssRNA, presumably due to possessing twice as many 5′ppp moieties (Figure S8). Interestingly, RIG-I CTD interacts with the RIG-I helicase linker region (420–627, Figure 3E), suggesting that this region retains the binding property of RD.

Structure of RIG-I CTD in Solution

The structure of CTD in solution was determined using NMR spectroscopy (Figure 4A, Figure S9, and Table 1). The core of the structure is formed by a β sheet comprised of six central antiparallel β strands (β3–8). Another antiparallel β sheet (β1, 2, 9) is located on top of the central β sheet and flanks α1 and α2 together with the central β sheet. The C-terminal region forms a long unwound structure, capping one end of the central β sheet with two α helices (α3, 4) (Figure 4B). The structure is maintained by hydrophobic interactions derived from residues on the surface of those secondary structures that are well conserved among its homologs, MDA5 and LGP2 (Figure 4B). The electrostatic surface revealed that RIG-I CTD has a large basic cleft parallel to the central β sheet (Figure 4C). One edge of the cleft is capped by two α helices (α2 and α3), and the other is capped by a flexible loop between β5 and β6. In contrast, the opposite surface of CTD contains acidic patches.

Despite poor sequence homology, RIG-I CTD is structurally similar to the mammalian suppressor of Sec4 (Mss4) according to searches using Dali (Figure 4D) (Holm and Sander, 1993). Mss4 is a guanine nucleotide exchange factor (GEF) essential for the activation of Rab family GTPases (Yu and Schreiber, 1995a, 1995b). Although the central β sheet and the capping three antiparallel β strands and two α helices were conserved in both structures, there are appreciable structural differences between them (Figure 4D). RIG-I CTD lacks the βA and β hairpin (βE, βF, and a connecting loop) in Mss4. The β hairpin covers the surface of the central β sheet and is involved in binding to Rab GTPase. In contrast, RIG-I CTD has a long C-terminal tail comprised of α3, α4, and a linker that surrounds the central β sheet. RIG-I CTD also has a long flexible loop between β5 and β6. Mss4 is known to have two CysXXCys motifs that act as a Zn^{2+}-binding site, thus stabilizing the structure. The first motif

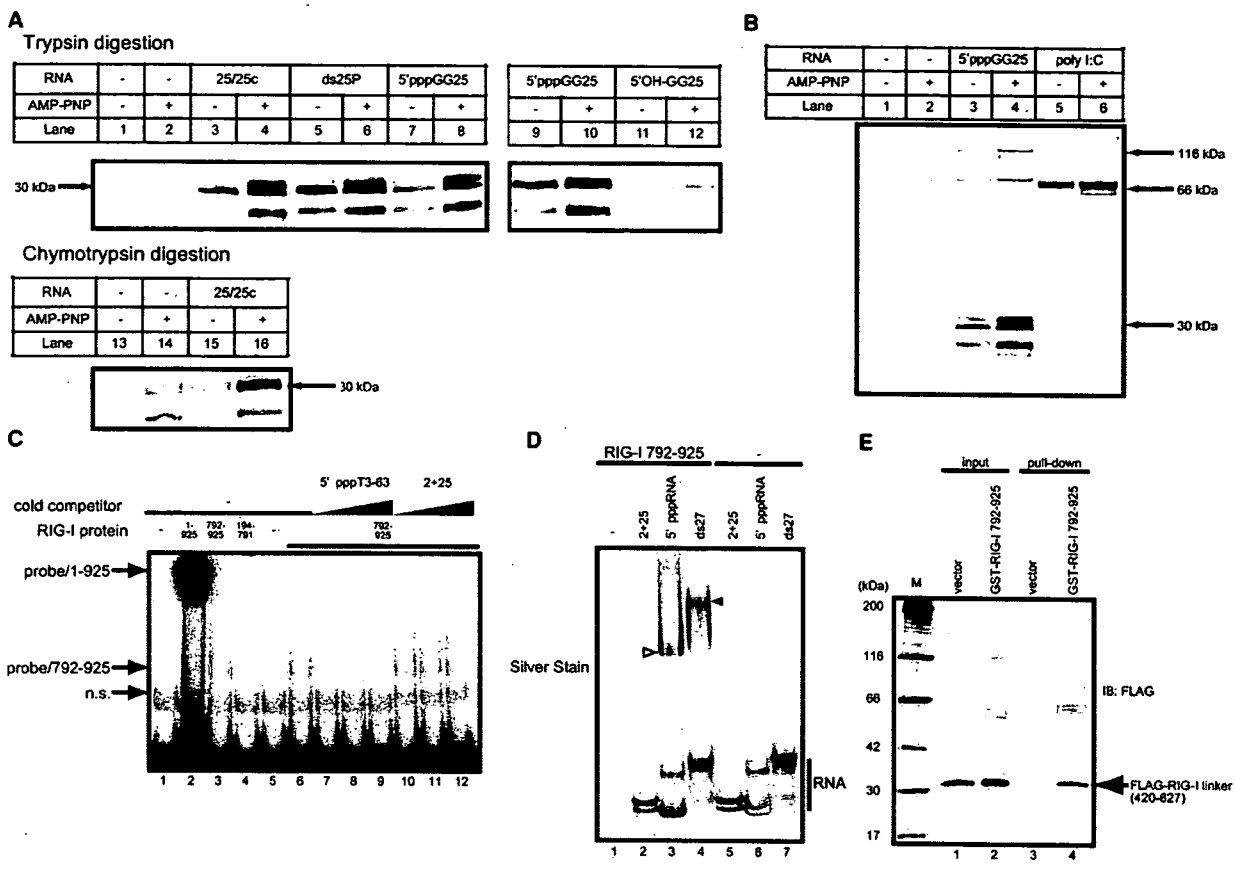

Figure 3. Conformational Change of RIG-I and Identification of CTD as the RNA Recognition Domain

(A) Protease digestion of RIG-I. RIG-I was incubated with the indicated RNA in the absence (odd number lanes) or presence of AMP-PNP (5 mM, even number lanes). The mixture was digested with trypsin (lanes 1–12) or with chymotrypsin (lanes 13–16). The digested RIG-I was analyzed by SDS-PAGE followed by anti-RIG-I immunoblotting.

(B) RIG-I was incubated with 5'ppp-GG25 or poly I:C and analyzed as in (A).

(C) Specific recognition of dsRNA and 5'ppp ssRNA by RIG-I 792–925. EMSA using a ^{32}P-labeled dsRNA probe (^{32}P-GG25/2+25c, 0.08 pmol) and either a full-length RIG-I (1–925, 30 pmol), or the C-terminal (792–925, 50 pmol) or helicase domain (194–925, 50 pmol) of RIG-I. Cold 5'ppp ssRNA (T3-63, lanes 7–9: 50, 100, and 200 pmol, respectively) or 5'OH ssRNA (ss2+25, lanes 10–12: 50, 100, and 200 pmol, respectively) was included. RIG-I/probe complexes are indicated. n.s., nonspecific band.

(D) RIG-I (792–925, 50 pmol) was mixed with 5'OH ssRNA (2+25, 100 pmol, lane 2) or 5'ppp ssRNA (T3-63, 100 pmol, lane 3) or dsRNA (ds27, 100 pmol, lane 4) and resolved in a 7.5% acrylamide gel and silver stained. The probe alone was electrophoresed as indicated (lanes 5–7). Triangles indicate RNA-protein complexes. Under these conditions, RIG-I (792–925) did not enter the gel (lane 1).

(E) Huh7 cells were transfected with the expression vector for Flag-RIG-I linker (420–627) and empty GST vector (lanes 1 and 3) or the expression vector for GST-RIG-I 792–925 (lanes 2 and 4). Cell extracts were subjected to pull-down assays using glutathione Sepharose beads and analyzed for immunoblotting (lanes 3 and 4) along with one-tenth the amount of crude extract (lanes 1 and 2, input) using anti-Flag. The position of the Flag-RIG-I linker is indicated.

is conserved in the RIG-I family, but the second motif has an insertion in RIG-I and a deletion in MDA5 (Figure 4B). We tested by atomic absorption spectrophotometer whether the solution structure of RIG-I CTD contains Zn^{2+} and found that RIG-I CTD roughly contains an equimolar amount of Zn^{2+} (Table S1). We compared the spectra with and without 50 mM EDTA (0.1 mM CTD, at 4°C for 7 days); however, negligible chemical shift perturbation was observed. On the other hand, Zn^{2+} was removed under denaturing condition (6 M guanidine hydrochloride) in the presence of 50 mM EDTA, as confirmed by atomic absorption experiments, suggesting that Zn^{2+} is involved in the structural integrity (Table S1).

Effect of Binding RNA on NMR Spectra

In order to investigate the binding surface for dsRNA, ssRNA, and 5'ppp ssRNA, NMR titration was performed with RNAs used in EMSA. A progressive decrease in intensity was observed in ^{1}H-^{15}N-HSQC spectra with the addition of either dsRNA or 5'ppp ssRNA (Figures 5A and 5B). A smaller decrease in intensity was also seen on titration with ssRNA. This indicates that the

Please cite this article in press as: Takahasi et al., Nonself RNA-Sensing Mechanism of RIG-I Helicase and Activation of Antiviral Immune Responses, Molecular Cell (2008), doi:10.1016/j.molcel.2007.11.028

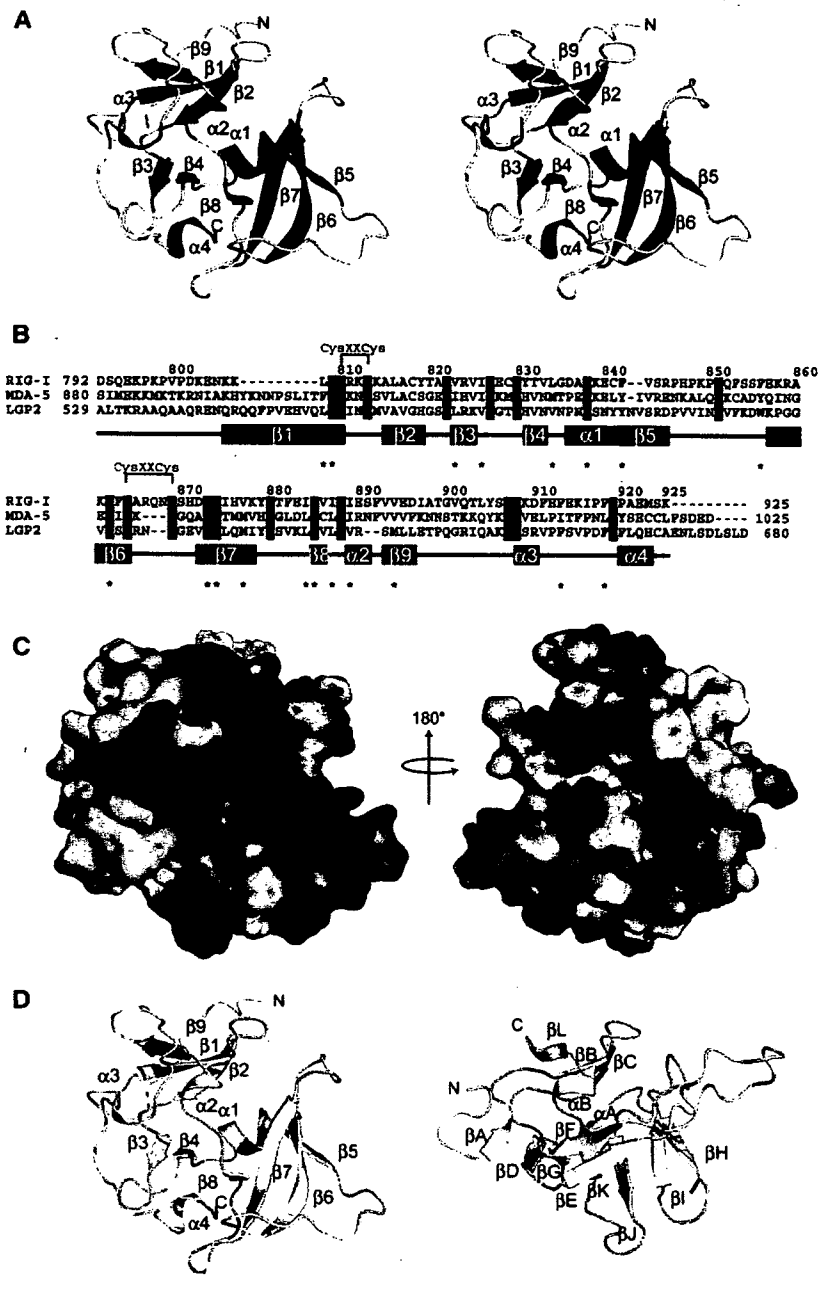

Figure 4. Structure of RIG-I CTD in Solution

(A) Stereo view of a ribbon diagram of the lowest-energy structure. Secondary structural elements are labeled.

(B) Sequence alignment of RIG-I CTD and its homologs human MDA5 and human LGP2. The secondary structural elements are indicated below the alignment. The amino acid in red and yellow indicates conserved and type-conserved residues, respectively. Conserved residues that participate in the hydrophobic core are indicated with asterisk (*). CysXXCys motifs are also indicated.

(C) The electrostatic surface potential of RIG-I CTD. Positive and negative electrostatic surfaces are in blue and red, respectively. Left, the model corresponds to the orientation of RIG-I CTD in (A). Right, surface potential of CTD rotated 180° along the vertical axis.

(D) Comparison of the structure of RIG-I CTD (left) and Mss4 (right). Structures are represented by a ribbon diagram. The structurally similar region between RIG-I CTD and MSS4 is shown in cyan, and other regions are shown in yellow. All of the figures were prepared using PyMOL (http://www.pymol.org).

formation of the protein/RNA complex is an intermediate exchange process on the NMR chemical shift timescale. The residues that disappeared were located on one surface of the protein, whereas the residues forming the opposite surface did not disappear, suggesting that the former residues participate in interaction with RNAs.

In dsRNA titration experiments, signals corresponding to the residues involved in a large cleft disappeared at 0.5 equivalents (molar ratio to RIG-I CTD). The cleft comprised β6 (Lys858 and Lys861), β7 (Asp872, Trp873, and Ile875), α2 (Ile889 and Glu890), and a flexible loop between β5 and β6 (Phe853 and Phe856). Notably, Lys858 and Lys861 are not conserved in RIG-I homologs, indicating that MDA5 and LGP2 would recognize viral RNAs in different ways. Other peaks, corresponding to Ile826 and Tyr879, also disappeared (Figure 5C). This cleft corresponds to the large basic cleft on the surface of RIG-I CTD (Figure 4C).

Surprisingly, titration with 5′ppp ssRNA showed a faster progressive decrease in intensity. Peaks responsible for binding with dsRNA also disappeared, such as β6 (Lys858, Ala860, and Lys861), β7 (Asp872, Trp873, Gly874, Ile875, His876, and Val877), α2 (Ile889 and Glu890), and the flexible loop between β5 and β6 (Phe853 and Phe856). In addition, residues on the adjacent surface formed by β4 (Tyr831), α2, and the loops between β3 and β4 (Ile826, Glu827, and His830), β7 and β8 (Tyr879), and the C-terminal tail containing α3 and α4 (Ser906, Trp908, and Lys915) disappeared with the addition of 0.25 equivalents of 5′ppp ssRNA. Residues Ala817, Val843, Arg845, Ile884, and Val893 also disappeared (Figure 5D).

These results imply that RIG-I CTD uses the large basic cleft along with the peripheral residues to recognize 5′ppp ssRNA and dsRNA. It is worth noting that the flexible loop between β5 and β6, which resides at one edge of the cleft, is conserved in MDA5 and LGP2. Likewise, residues Tyr831, Trp873, Gly874, Ile887, Lys888, Lys907, and Trp908, which reside at the other end of the cleft, are also conserved (Figures 4B and 5E).